Nukleon-Nukleon-Wechselwirkung, SS 2008

9. Vorlesung, 10.06.2008

Prof. Dr. E. Grosse

Nukleon-Nukleon-Wechselwirkung und van der Waals Kraft

Können die Eigenschaften schwerer Kerne berechnet werden?

Nukleonen und Kerne im elektromagnetischen Feld

Reziprozität: e.m. Zerfall und e.m. Anregung

Experimente mit Photonen - Riesenresonanzen

Astrophysik: Kerne in heißen Sternen

van der Waals force

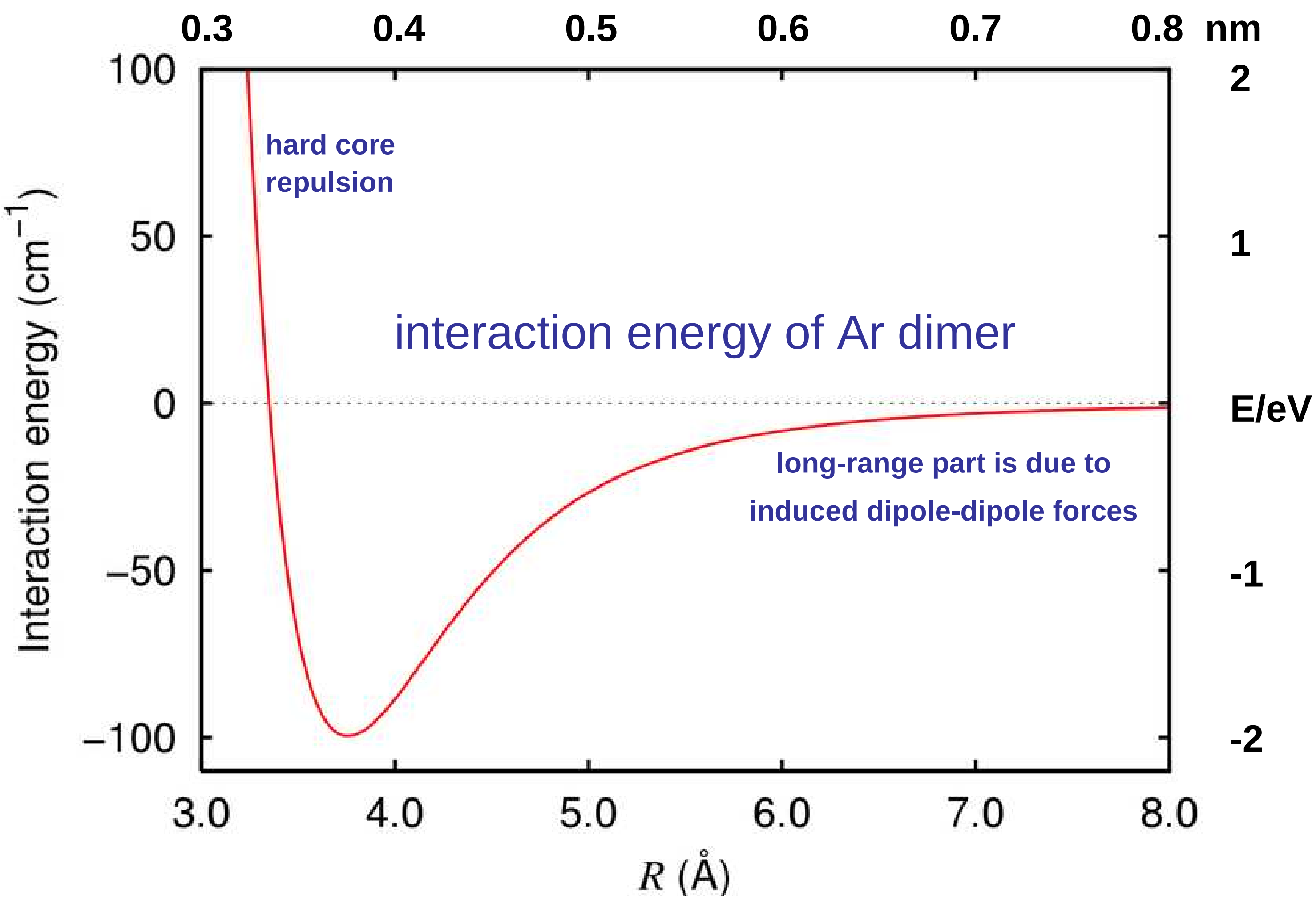

after Wikipedia®

Within the … Kohn-Sham DFT (density functional theory) , the … many-body problem of interacting *particles* in a static external potential is reduced to *the simpler* problem of non-interacting *particles* moving in an effective potential.

The effective potential includes the external potential and … the exchange and correlation interactions …..

An approximation is the local-density approximation (LDA), … which can be obtained from the Thomas-Fermi model…

Walter Kohn (* March 9, 1923 in Vienna, Austria), *University of California at Santa Barbara.*
He was awarded, with John Pople, the Nobel Prize in chemistry in 1998, *for*
… their contributions to the understandings of the .. properties of materials.
… Kohn played the leading role in the development of the density functional theory, which made it possible to incorporate quantum mechanical effects in the … density (rather than through its many-body wavefunction).
This computational simplification led to many insights and became an essential tool for *materials research, plasma theory,* atomic, molecular and *nuclear* structure .

cf.: E. K. U. Gross and R. M. Dreizler, *Density Functional Theory*, Plenum 1993

after Wikipedia®

Traditional methods in .. *many particle* theory, in particular Hartree-Fock theory and its descendants, are based on the complicated many-*body* wavefunction.

The main objective of density functional theory is to replace the many-body .. wavefunction with the .. density as the basic quantity.

Whereas the many-body wavefunction is dependent on 3N variables,
three spatial variables for each of the N *particles*,
the density is only a function of *3 coordinates* and is *much* simpler … Wikipedia®

One thus has to use a particle-particle potential which is density dependent and thus cannot be directly measured in particle-particle collisions.

But it can be constructed on the basis of particle-particle data by introducing a 'natural' density dependence, i.e. many body effects.

The pion exchange potential (Yukawa) of nuclear physics has a straightforward many body property:

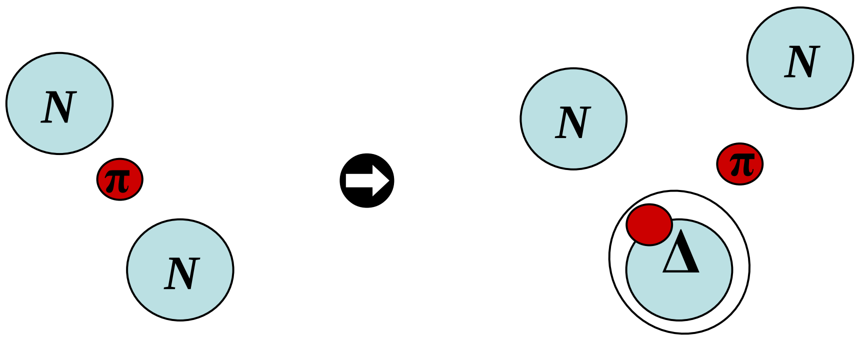

$\Delta : \Delta(1232\ MeV)$

$\Gamma_\Delta \sim 120\ MeV$

$\tau_\Delta \sim 5.5\ 10^{-24}\ s$

$\triangleq 1.6\ fm/c$

meson exchange

in quark picture

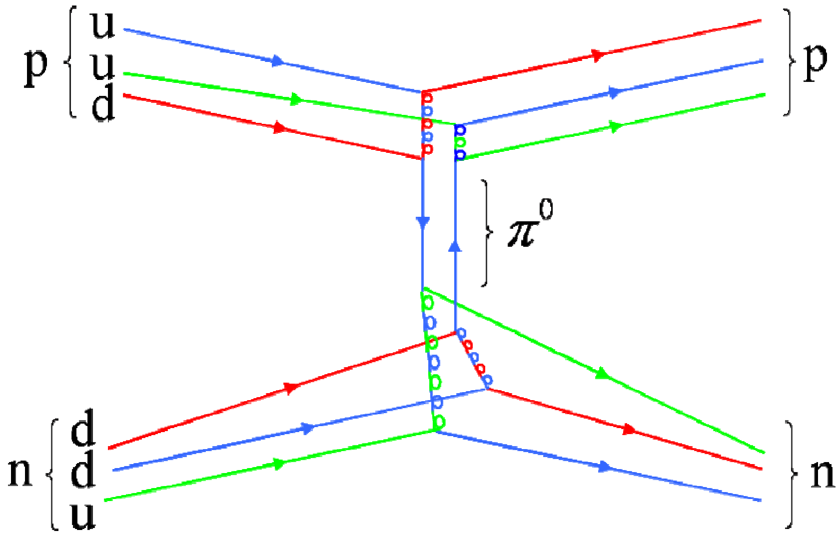

as Feynman diagram

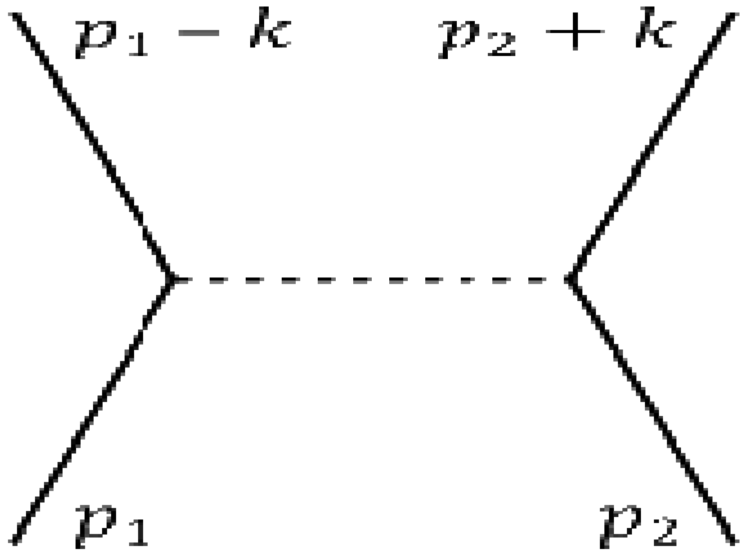

$$V(r) = -g^2 \frac{e^{-mr\frac{c}{\hbar}}}{r} \quad \leftarrow \quad \textbf{Fourier transform} \quad \rightarrow \quad V(\mathbf{k}) = -g^2 \frac{4\pi}{k^2 + m^2}$$

after Wikipedia®

Schematic meson-exchange-potential

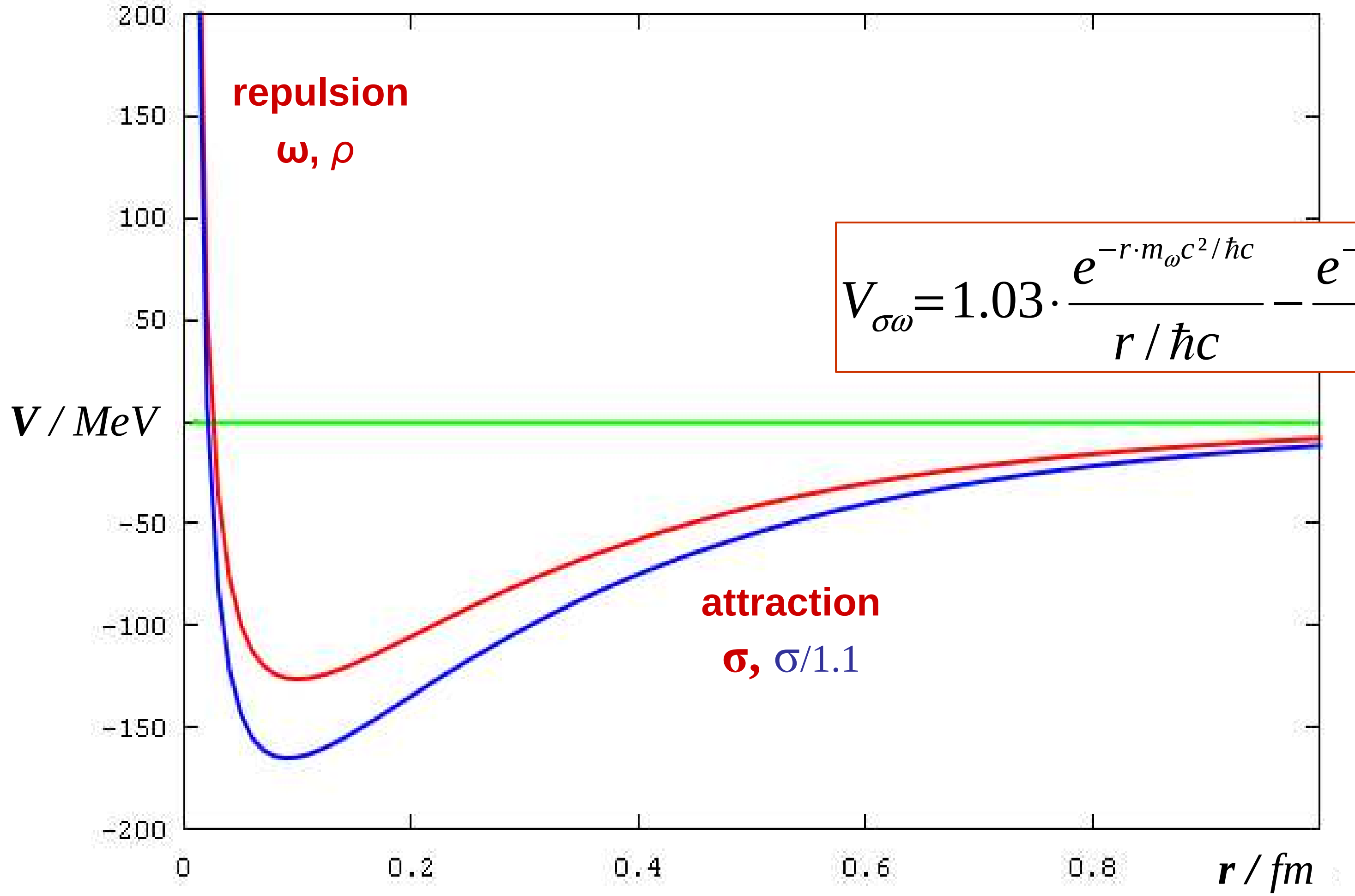

$$V_{\sigma\omega} = 1.03 \cdot \frac{e^{-r \cdot m_\omega c^2/\hbar c}}{r/\hbar c} - \frac{e^{-r \cdot m_\sigma c^2/\hbar c}}{r/\hbar c}$$

$m_\sigma c^2 = 550\ MeV$

$m_\rho c^2 = 763\ MeV$

$m_\omega c^2 = 783\ MeV$

Peter Ring, Elena Litvinova et al.,
München + Erice, Sept. 2006

Walecka model ➡ $\boxed{E[\rho]}$

Nucleons are coupled by exchange of mesons through an effective Lagrangian (EFT)

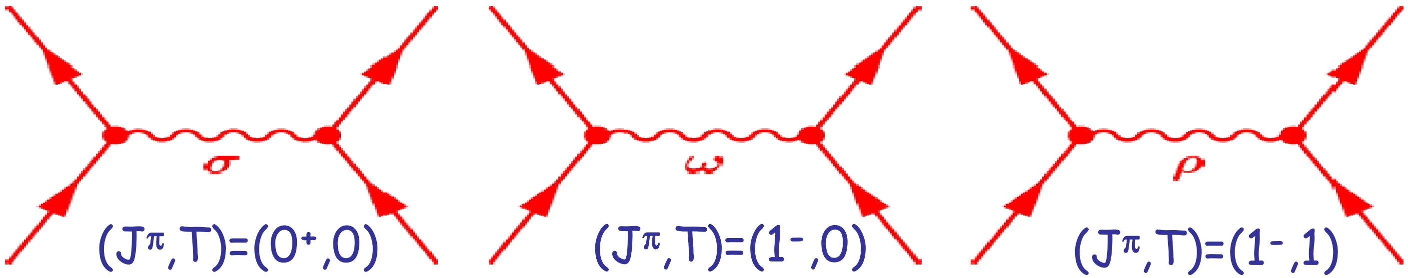

$$S(\mathbf{r}) = g_\sigma \sigma(\mathbf{r}) \qquad V(\mathbf{r}) = g_\omega \cdot \omega(\mathbf{r}) + g_\rho \cdot \vec{\tau}\vec{\rho}(\mathbf{r}) + e \cdot A(\mathbf{r})$$

Sigma-meson: attractive scalar field	Omega-meson: short-range repulsive	Rho-meson: isovector field	Coulomb field

cf.: G. A. Lalazissis, P. Ring, and D. Vretenar, *Extended Density Functionals in Nuclear Structure Physics*, Lecture Notes in Physics 641 (Springer-Verlag, Berlin/Heidelberg, 2004).

Single particle spectrum in ^{208}Pb ± 1 nucleon

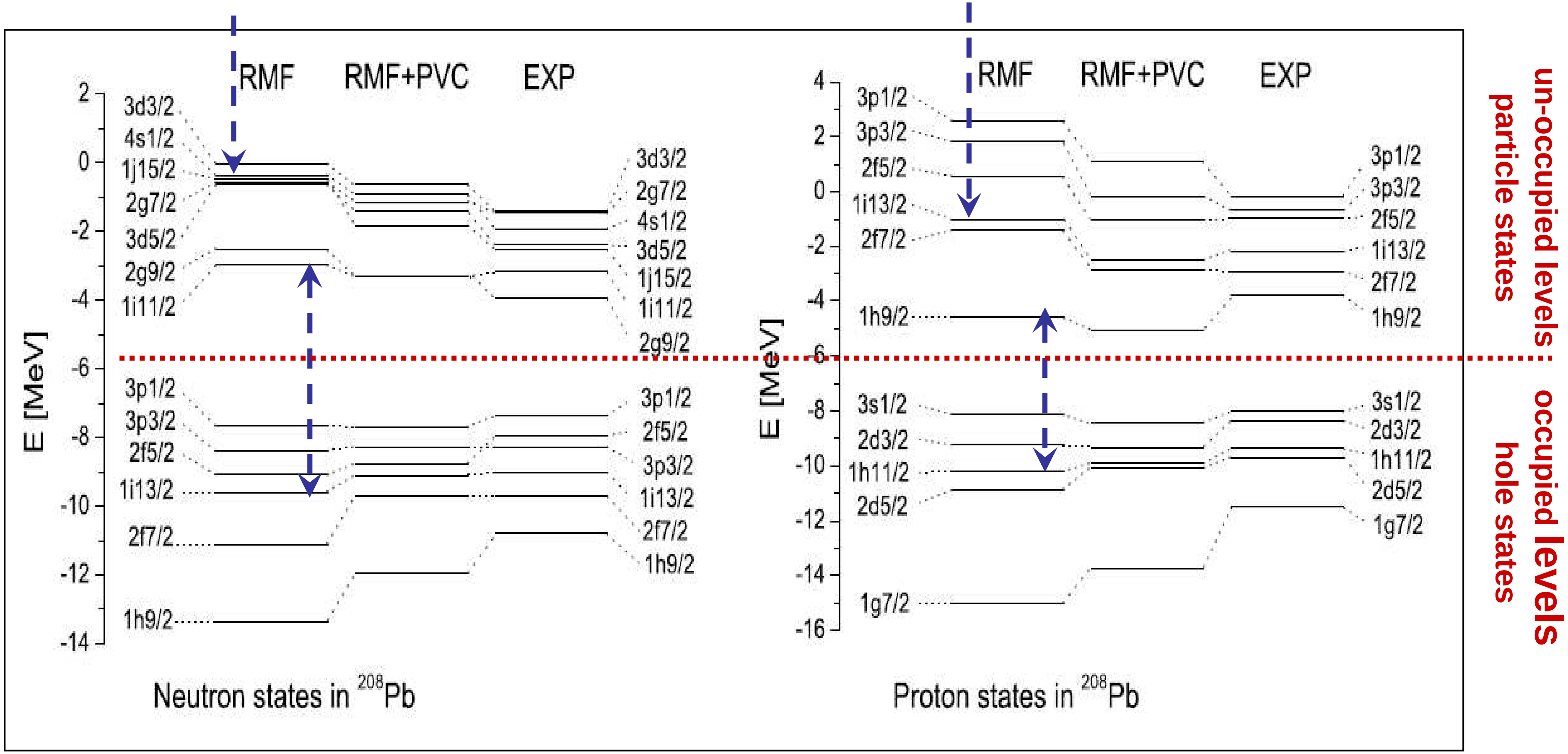

E. Litvinova and P. Ring, PRC 73, 44328 (2006)

In this covariant theory the spin orbit splitting is obtained without a special ℓs-term; thus the magic numbers come out as observed in the data.

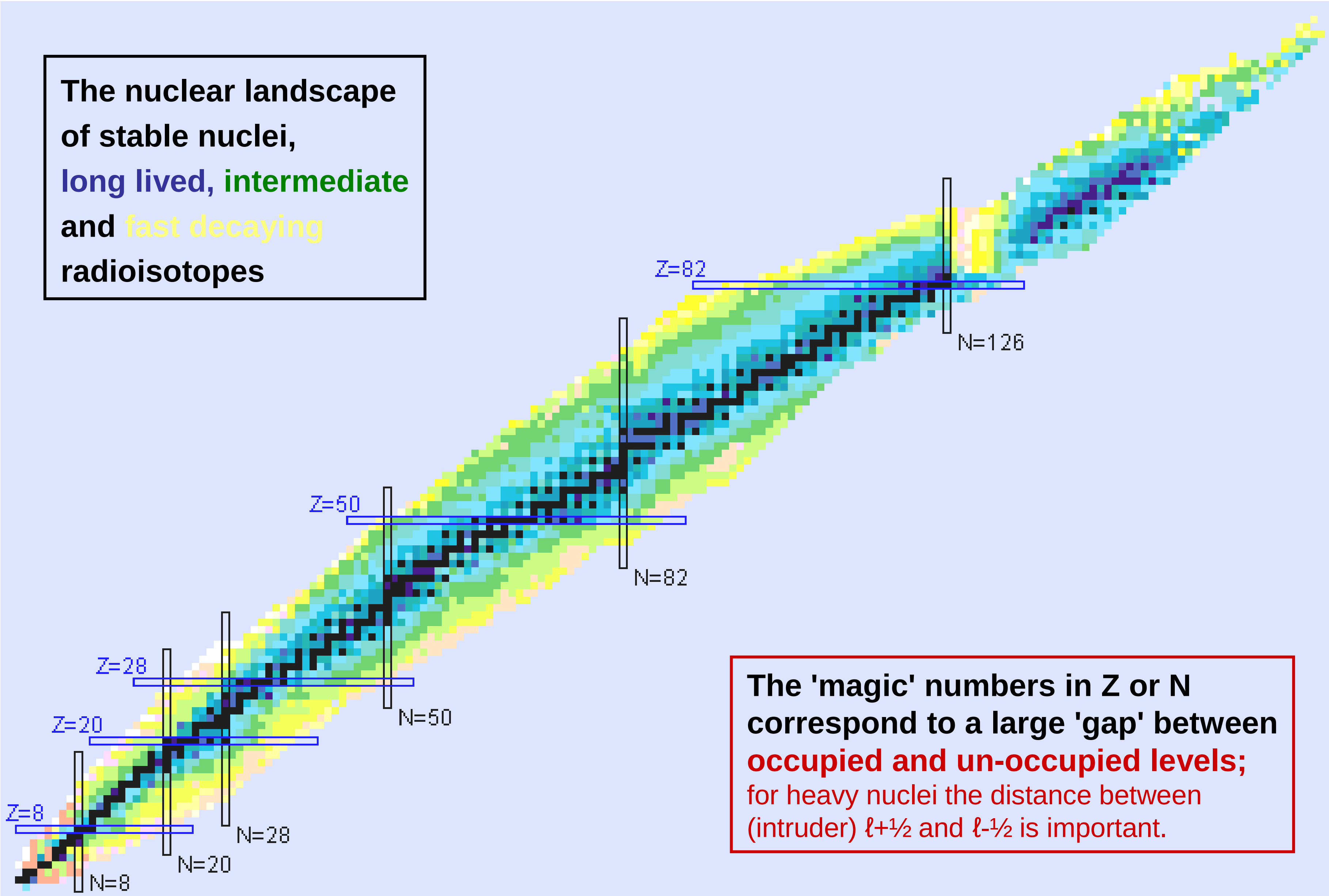
The nuclear landscape
of stable nuclei,
long lived, intermediate
and fast decaying
radioisotopes
Z=82
N=126
Z=50
N=82
Z=28
Z=20
Z=8
N=50
N=28
N=20
N=8
The 'magic' numbers in Z or N
correspond to a large 'gap' between
occupied and un-occupied levels;
for heavy nuclei the distance between
(intruder) ℓ+½ and ℓ-½ is important.

The effective nucleon-nucleon interaction is fixed by fitting to masses of many nuclei.

The meson-nucleon couplings g_σ, g_ω, g_ρ are assumed to be functions of the baryon density $\psi^\dagger\psi$ such that 8 independent parameters are adjusted (7 coupling parameters and the mass of the σ)

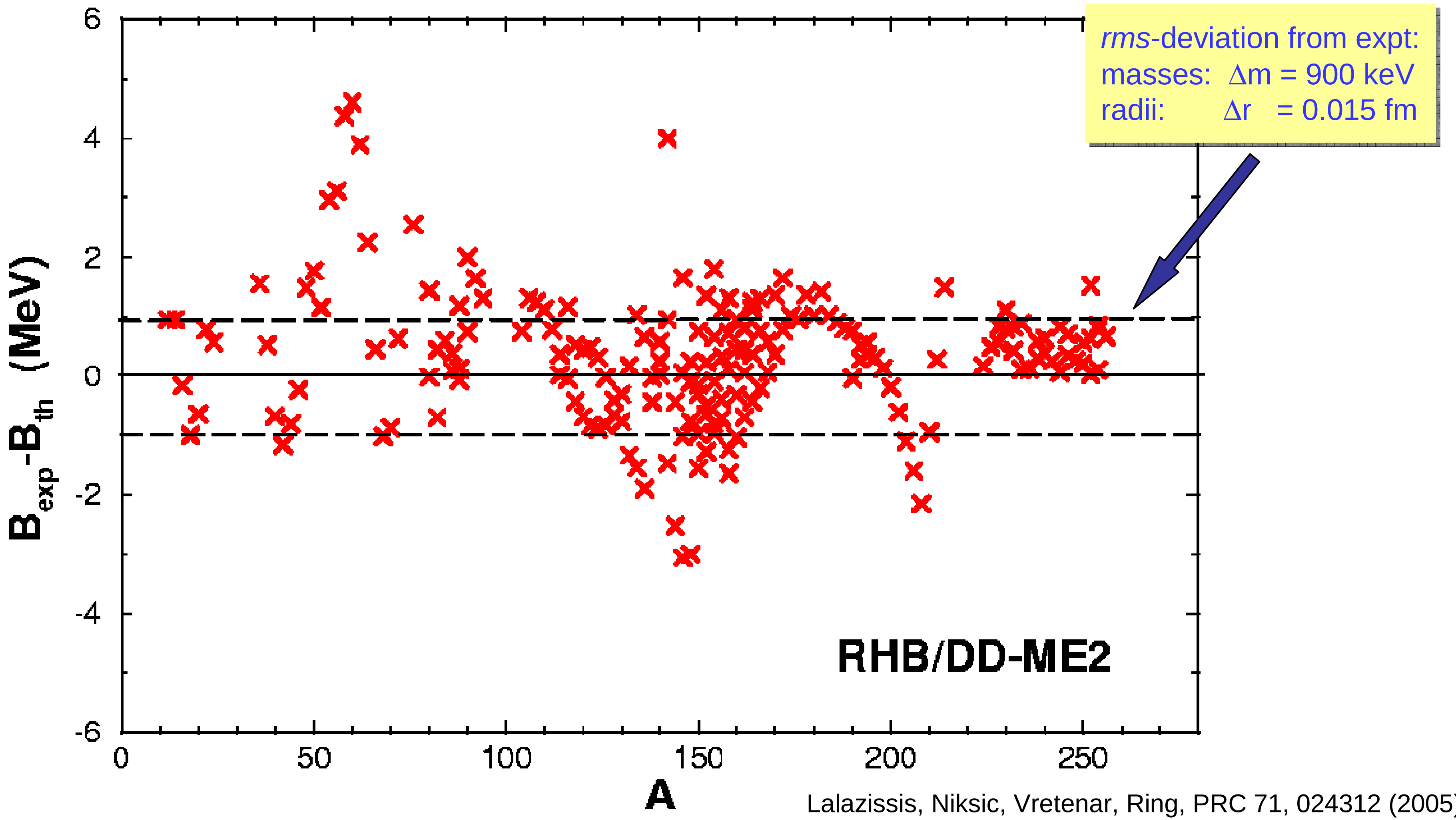

Lalazissis, Niksic, Vretenar, Ring, PRC 71, 024312 (2005)

Massenmessung im Speicherring

a) für heiße Strahlen bei
der transition energy

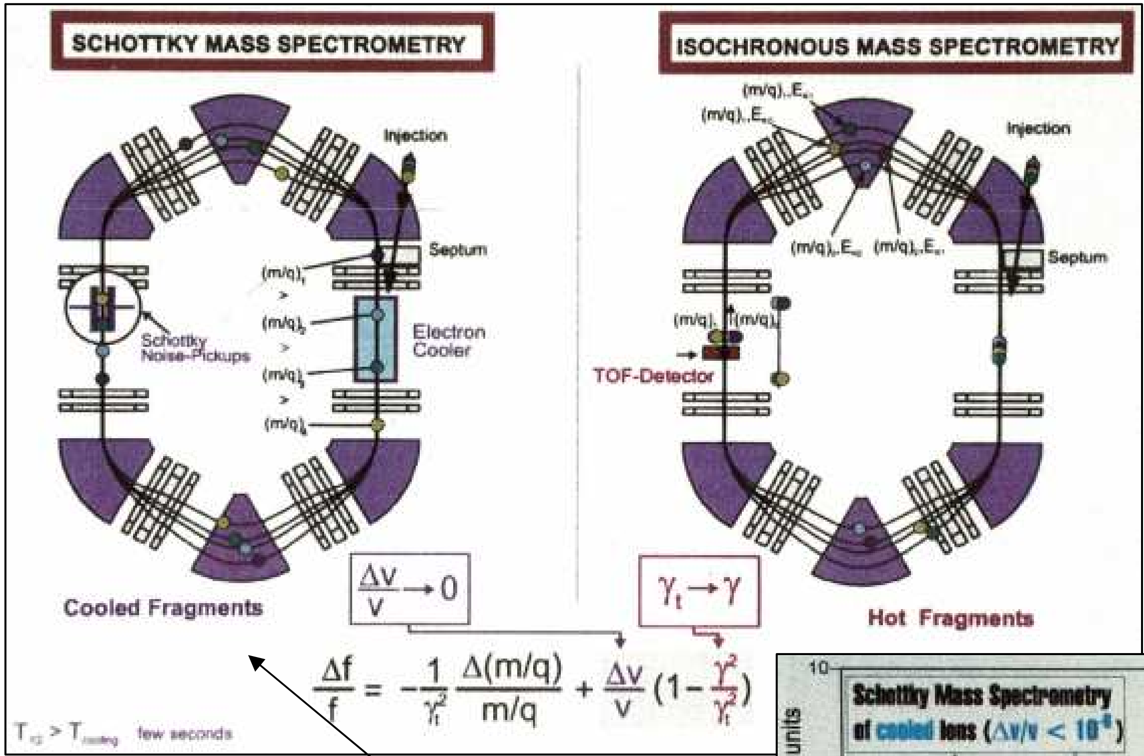

b) für gekühlte Strahlen
mit der sehr empfindlichen
Schottky-Methode

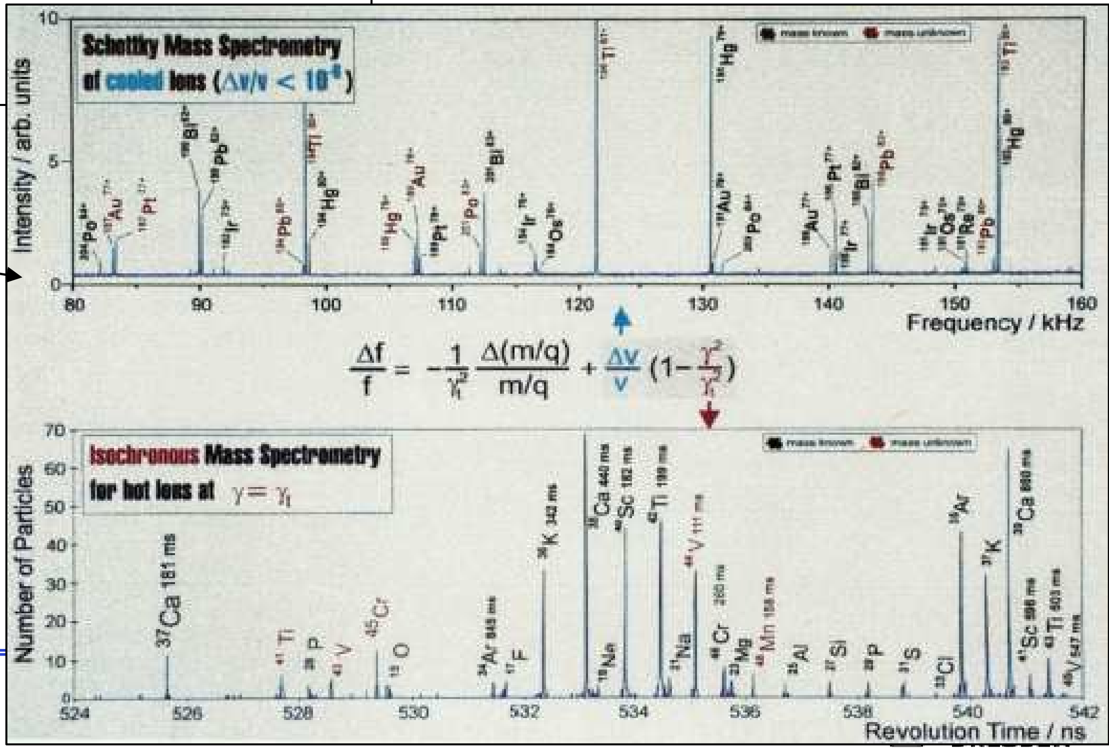

Neuartige Massenbestimmung in einer Hochfrequenzfalle

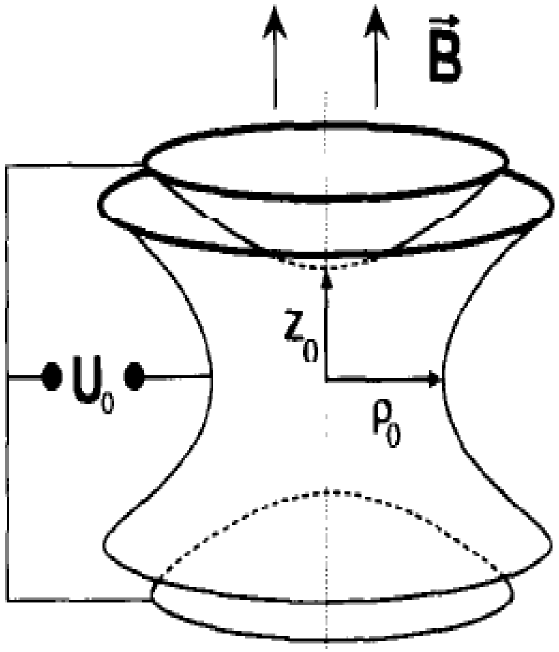

Fig. 1. Layout of a Penning trap. ρ_0 denotes the inner radius of the ring electrode and z_0 the half distance between the endcap electrodes.

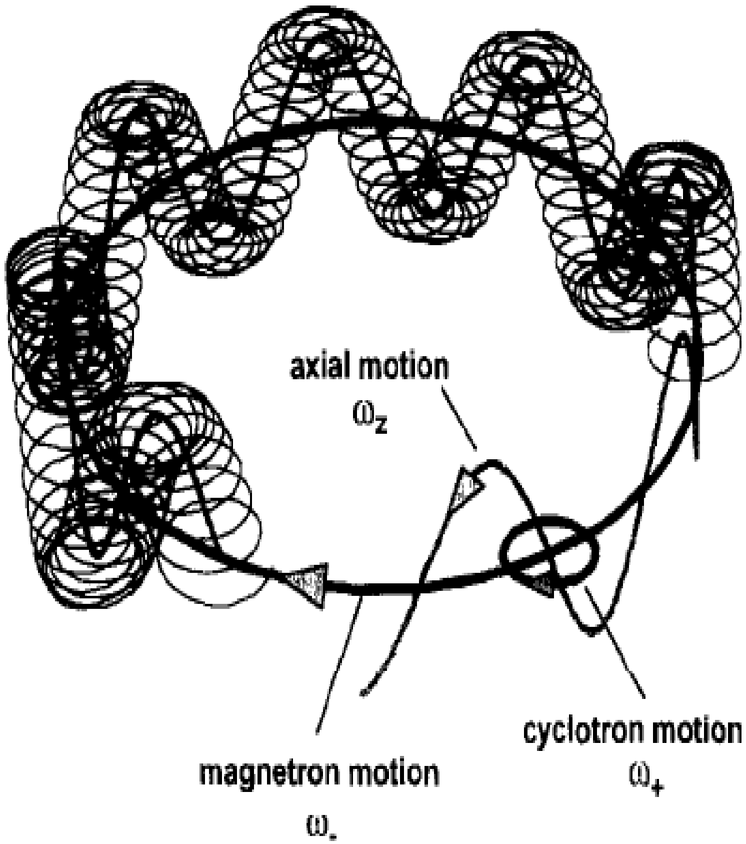

Fig. 2. Schematic of the three eigenmotions of an ion in a Penning trap.

Eichung mit Fulleren - nano-Partikeln

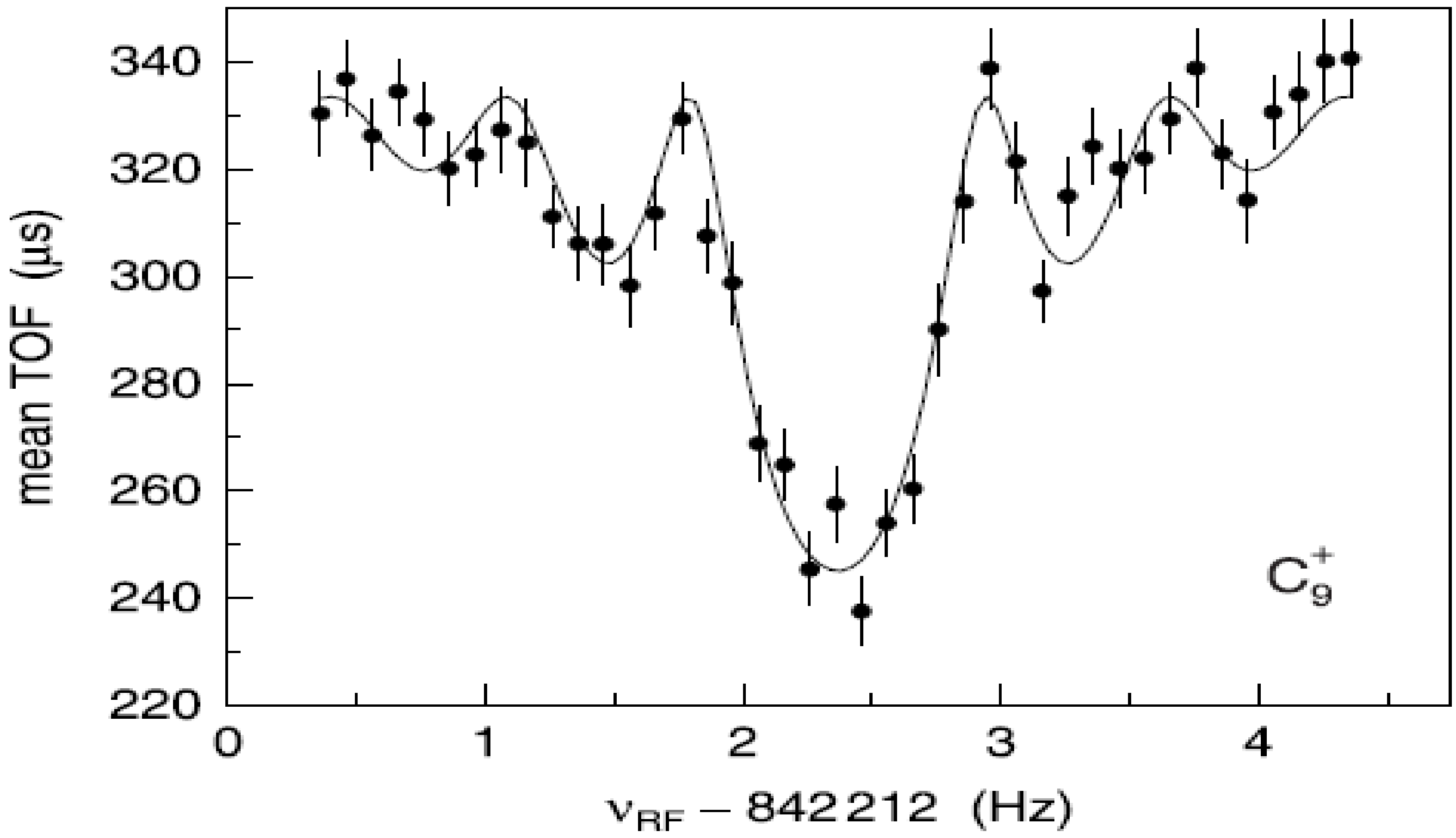

Fig. 3. Time-of-flight resonance curve of C_9^+. The solid line is a fit of the expected line shape to the data points [24]. The reduced χ^2 of the least-squares fit of the complete resonance is close to one.

Eichung mit Fulleren - nano-Partikeln

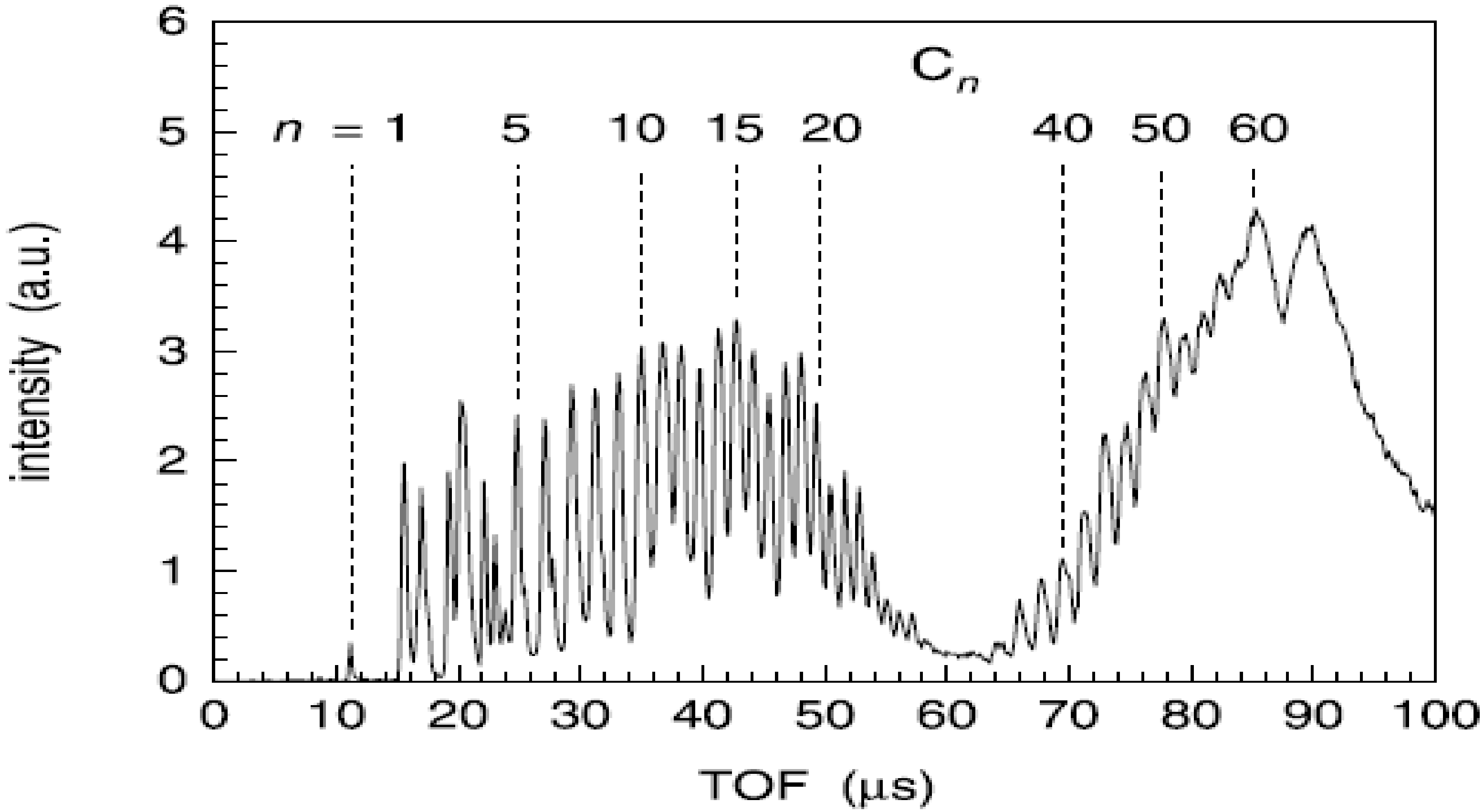

Fig. 2. Time-of-flight mass spectrum of carbon cluster ions produced by use of laser-induced desorption, fragmentation, and ionization of C_{60} at 532 nm at a laser pulse energy of about 10 mJ, recorded at MCP 1 [17]. The peak around $n = 70$ is probably due to coalescence products of C_{60} and smaller fragments.

HIGH-PRECISION MASS MEASUREMENTS OF EXOTIC NUCLEI WITH THE TRIPLE-TRAP MASS SPECTROMETER ISOLTRAP

K. Blaum et al., 2002
CERN-INTC/2002-021

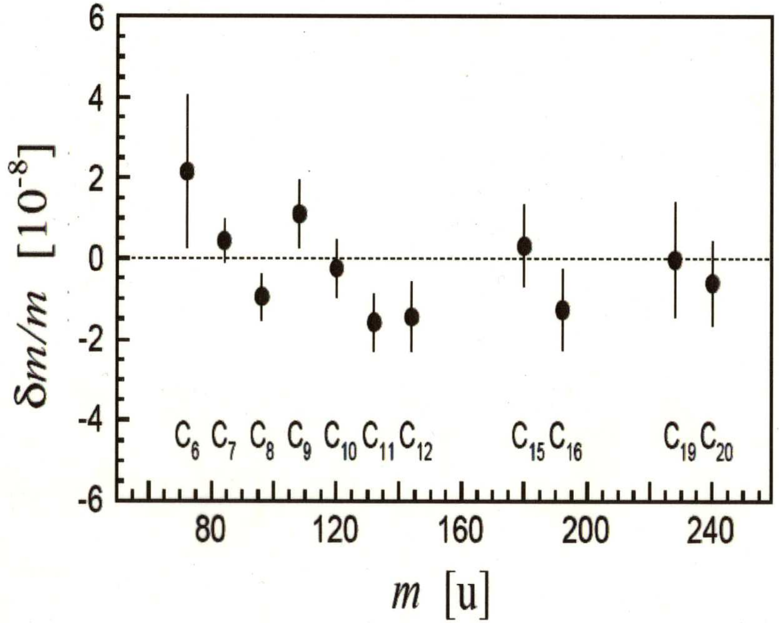

Figure 2: Weighted means of the cyclotron frequency ratios for all carbon cluster cross-reference measurements after taking all known systematic effects into account.

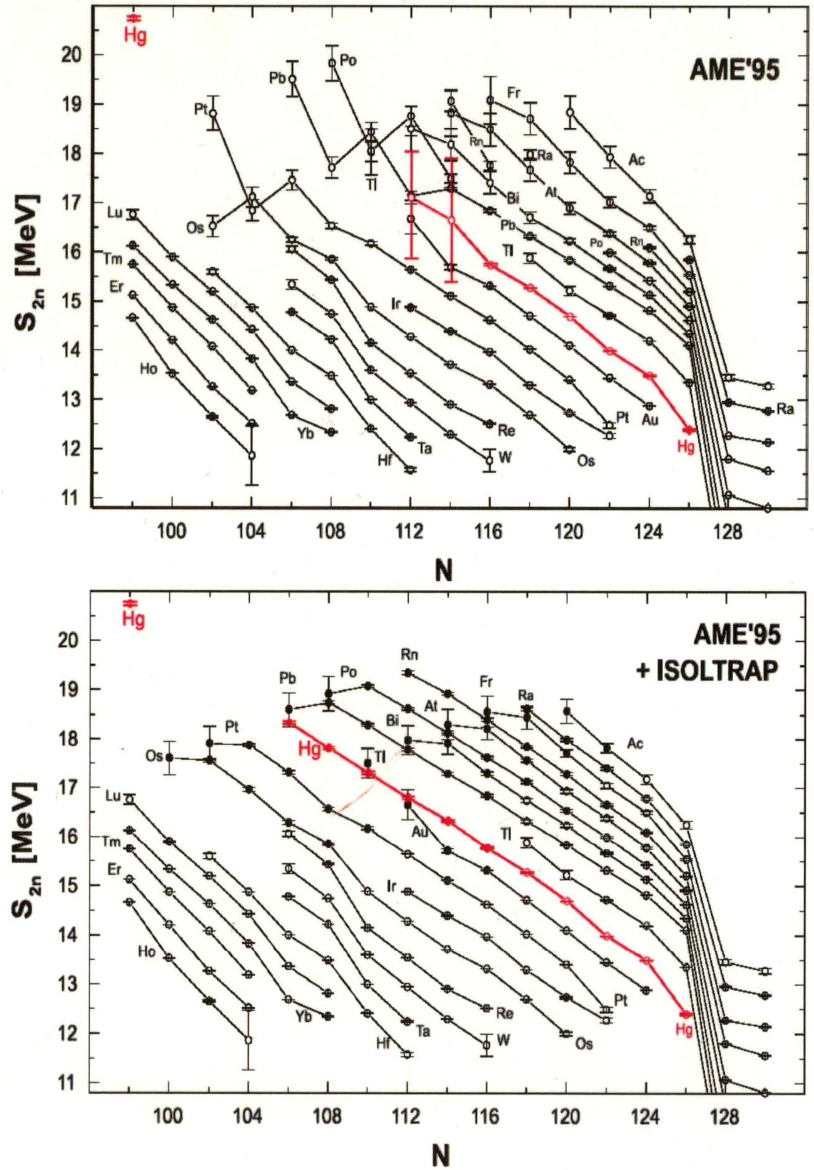

Figure 3: Two-neutron separation energies in the vicinity of $Z = 82$ as a function of neutron number. Shown are S_{2n} values excluding (top) and including (bottom) ISOLTRAP data in the atomic mass evaluation.

REXTRAP principle

magnetic field	3 T
cycle time	10 ms
buffer gas pressure	10^{-3} mbar

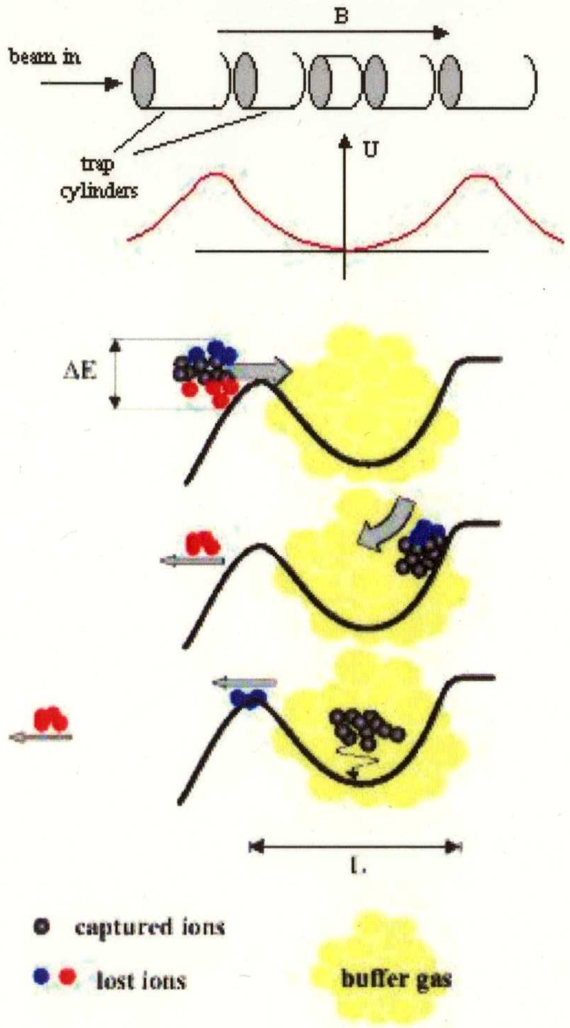

sideband cooling method

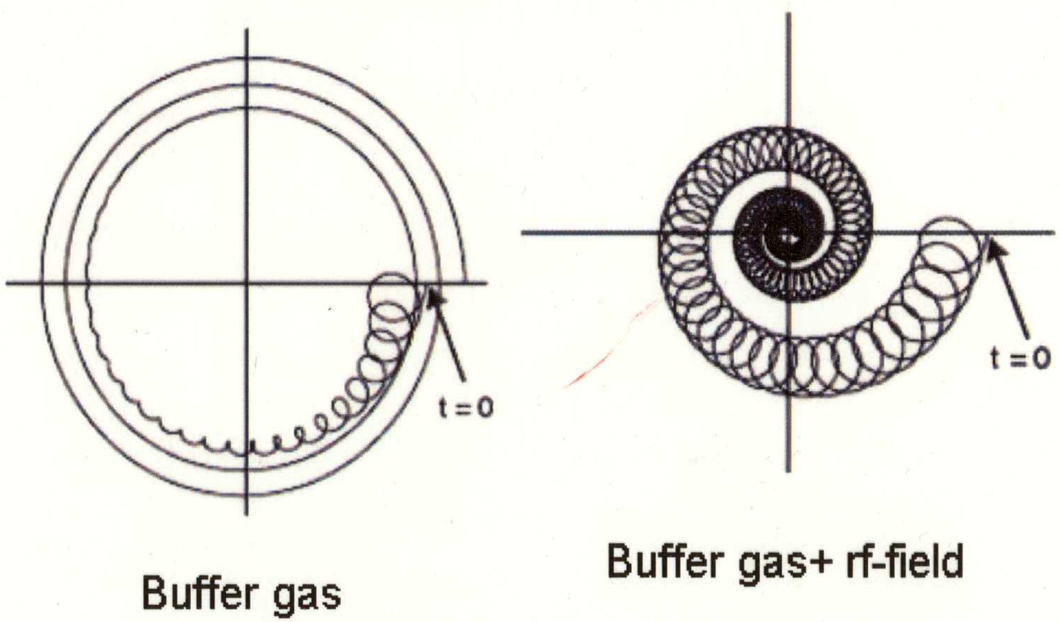

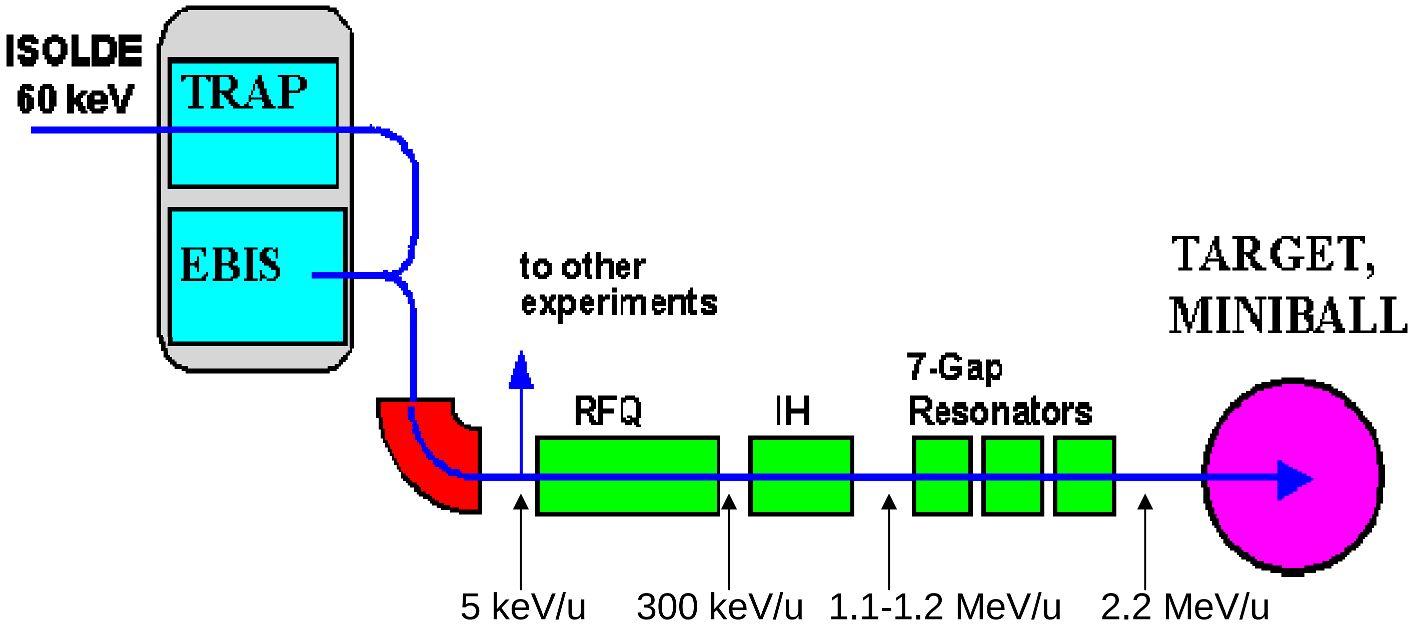

Aufbau am ISOLDE-Strahl radioaktiver Kerne, die im CERN-PS erzeugt werden

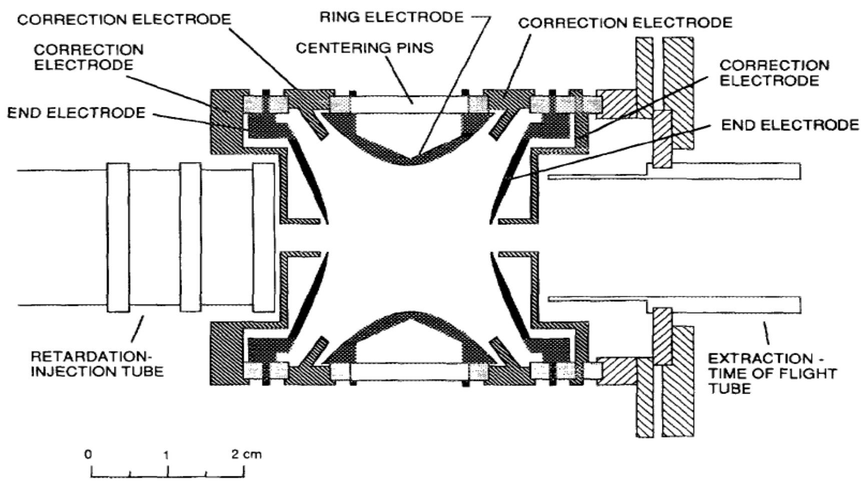

Nuclear energy surface

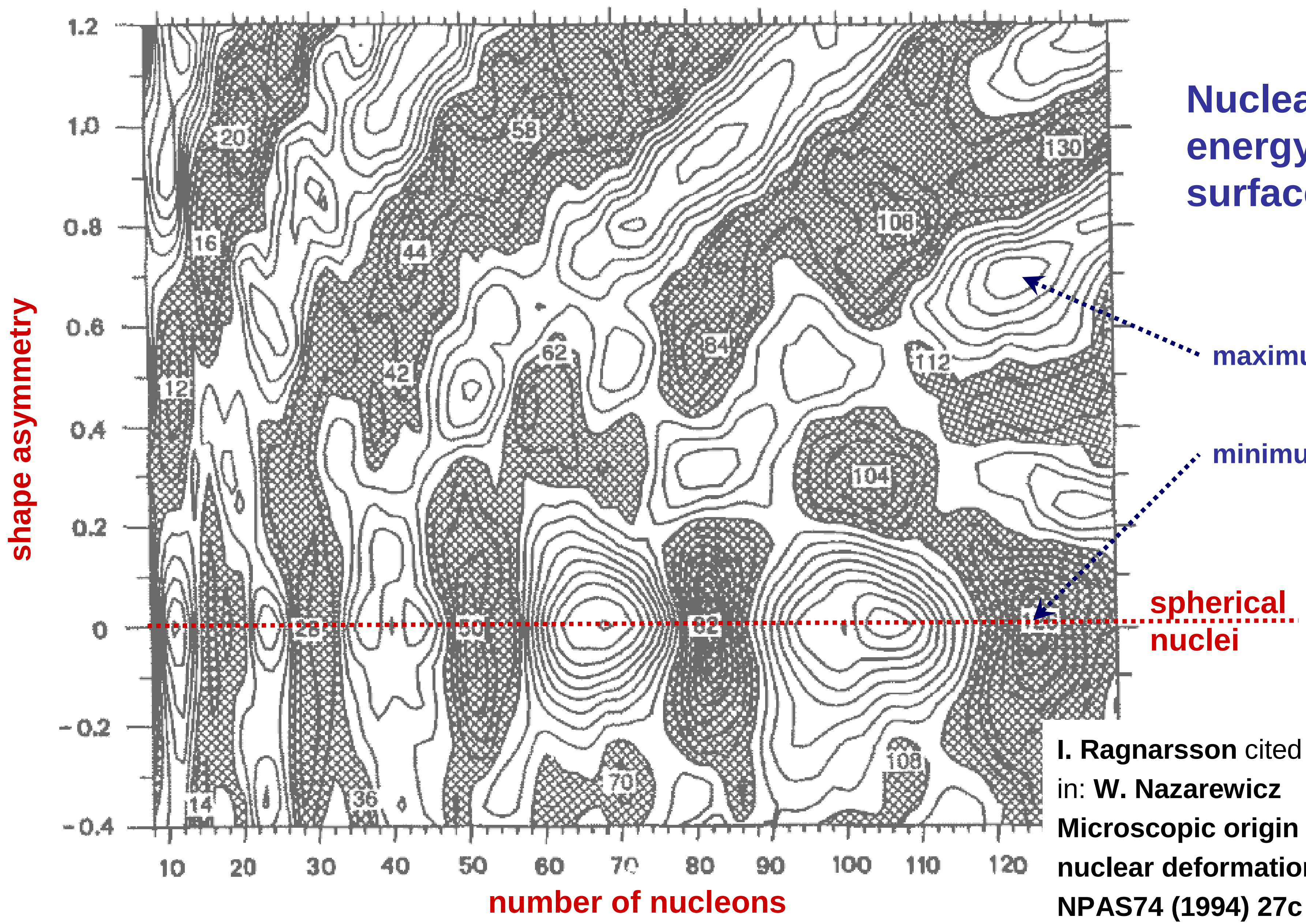

I. Ragnarsson cited in: **W. Nazarewicz Microscopic origin of nuclear deformations NPAS74 (1994) 27c**

Das DFT- Verfahren wurde bisher erfolgreich durchgeführt
nur für Kerne nahe abgeschlossener Schalen.

Außerhalb ist die sphärische Symmetrie verletzt und
die Rechnungen konnten bisher nicht voll durchgeführt werden.

Zur Berüchsichtigung der Deformation werden als Alternative
makroskopische Modelle (liquid drop, droplet) verwendet.

Die Kernmaterie wird wie eine Flüssigkeit behandelt mit
Volumenenergie (Kohäsion), Oberflächenspannung etc.

(vgl. Bethe-Weizsäcker Formel)

Üblich sind hybride Modelle, bei denen makroskopische und
mikroskopische Freiheitsgrade gemeinsam minimiert werden.

(Schaleneffekte: Strutinski-Verfahren)

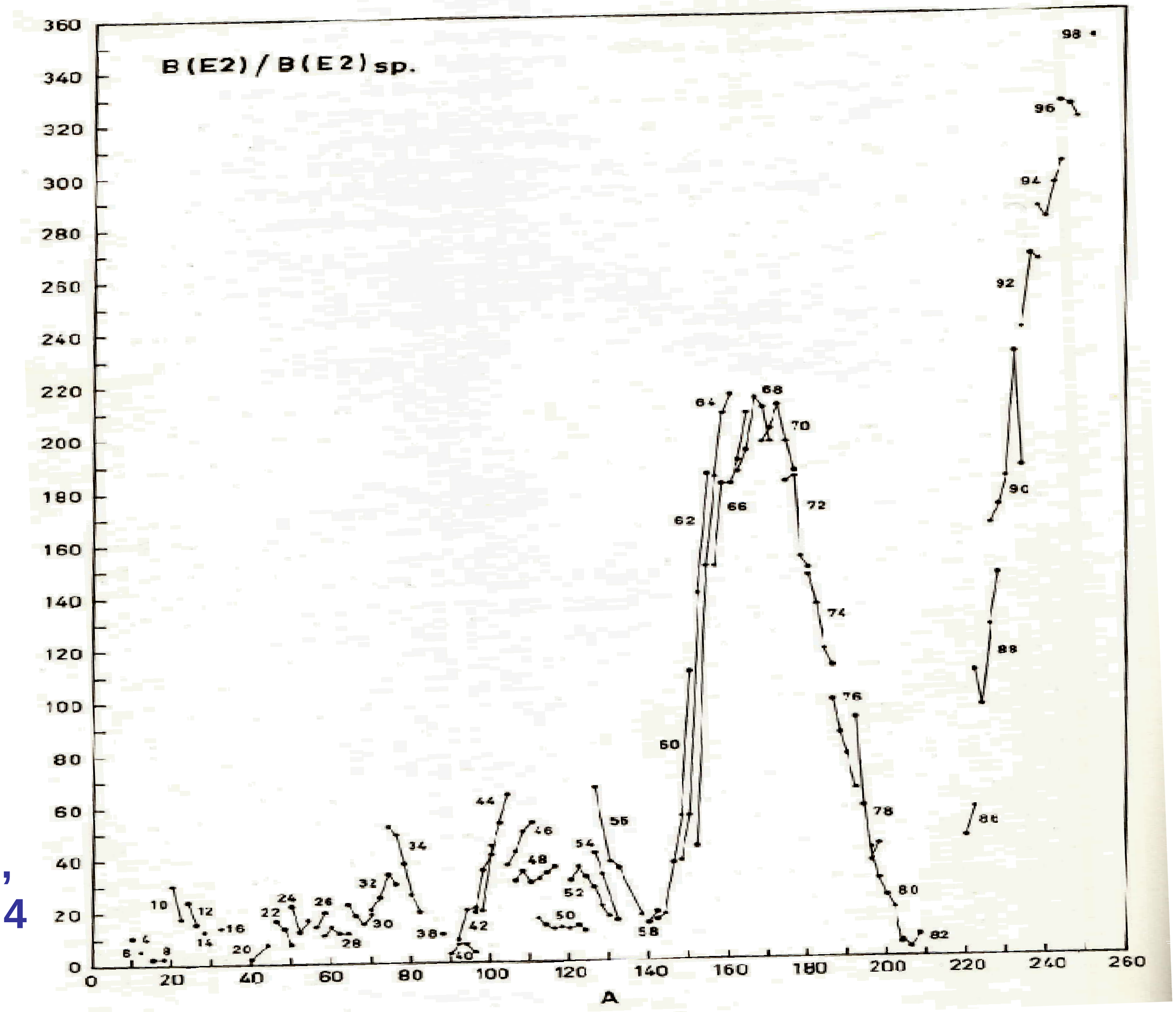

A. Bohr & B. Mottelson, Structure of Nuclei, ch 4
Rotational spectra

Experimentell wurde die Kerndeformation erschlossen aus:

1. Quadrupolmomenten ← Hyperfeinstruktur at. Linien

2. Energiedifferenzen in 'Rotations-banden'

beobachtet im α-Zerfall, Compoundkern-Zerfall

Quadrupol-Deformation

3. Coulombanregung solcher Banden

4. Lebensdauern von Niveaus in solchen Banden

3, 4 → Elektromagnetische Übergangswahrscheinlichkeiten

5. Form der Dipol-Riesenresonanz *dynamische* ***Dipol-Deformation***

Entscheidende Information liefert die Wechselwirkung mit elektromagnetischer Strahlung, die auf die (evtl. zeitabhängige**) Verteilung der Ladung** (Protonen) **empfindlich ist.**

Coulombanregung klassisch

im cm-Sytem, angeregt werden können

beide Stoßpartner, Target und Projektil

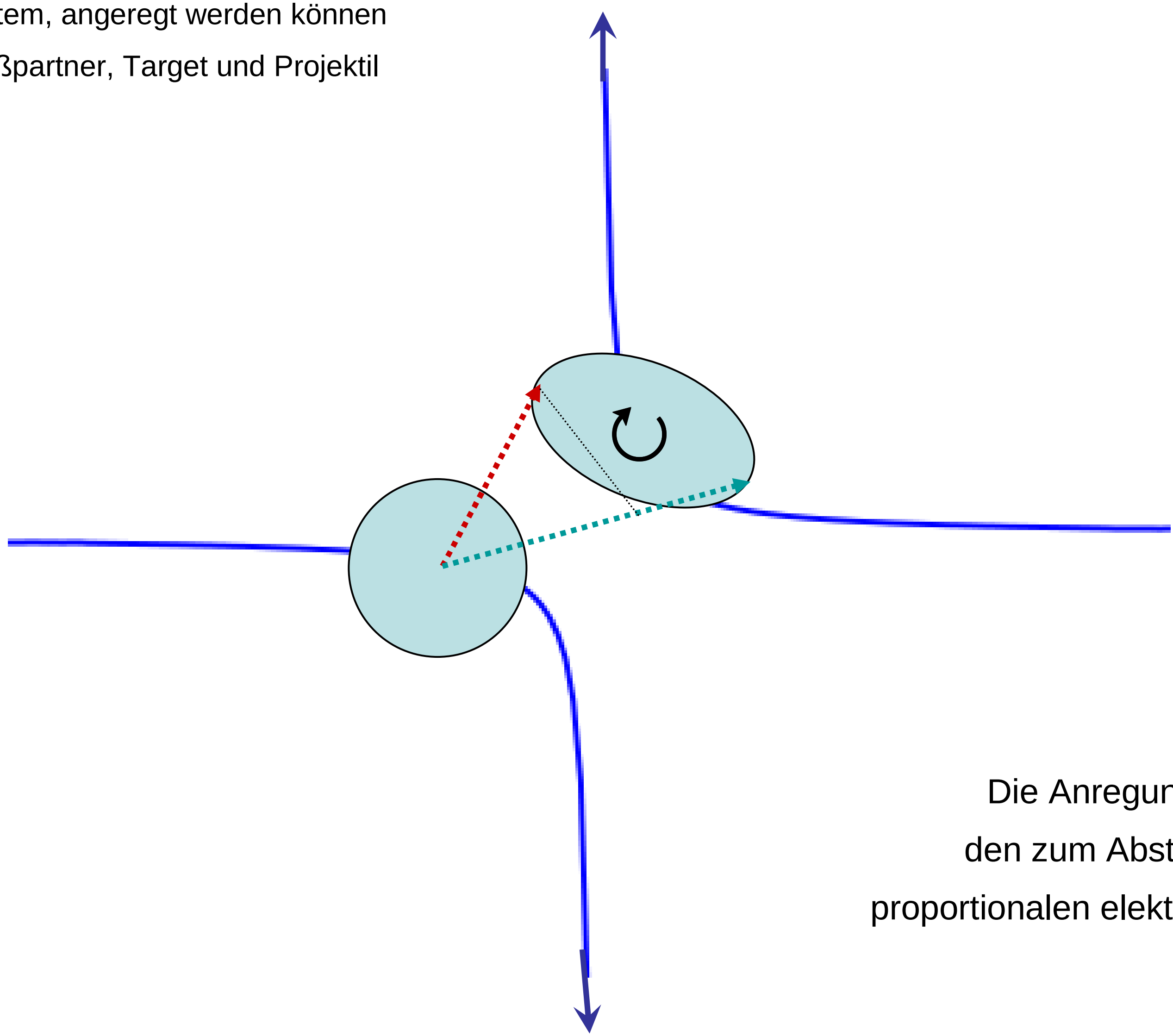

Die Anregung resultiert aus

den zum Abstand umgekehrt

proportionalen elektrischen Kräften

Coulombanregung quantenmechanisch

im cm-Sytem, angeregt werden können

beide Stoßpartner, Target und Projektil

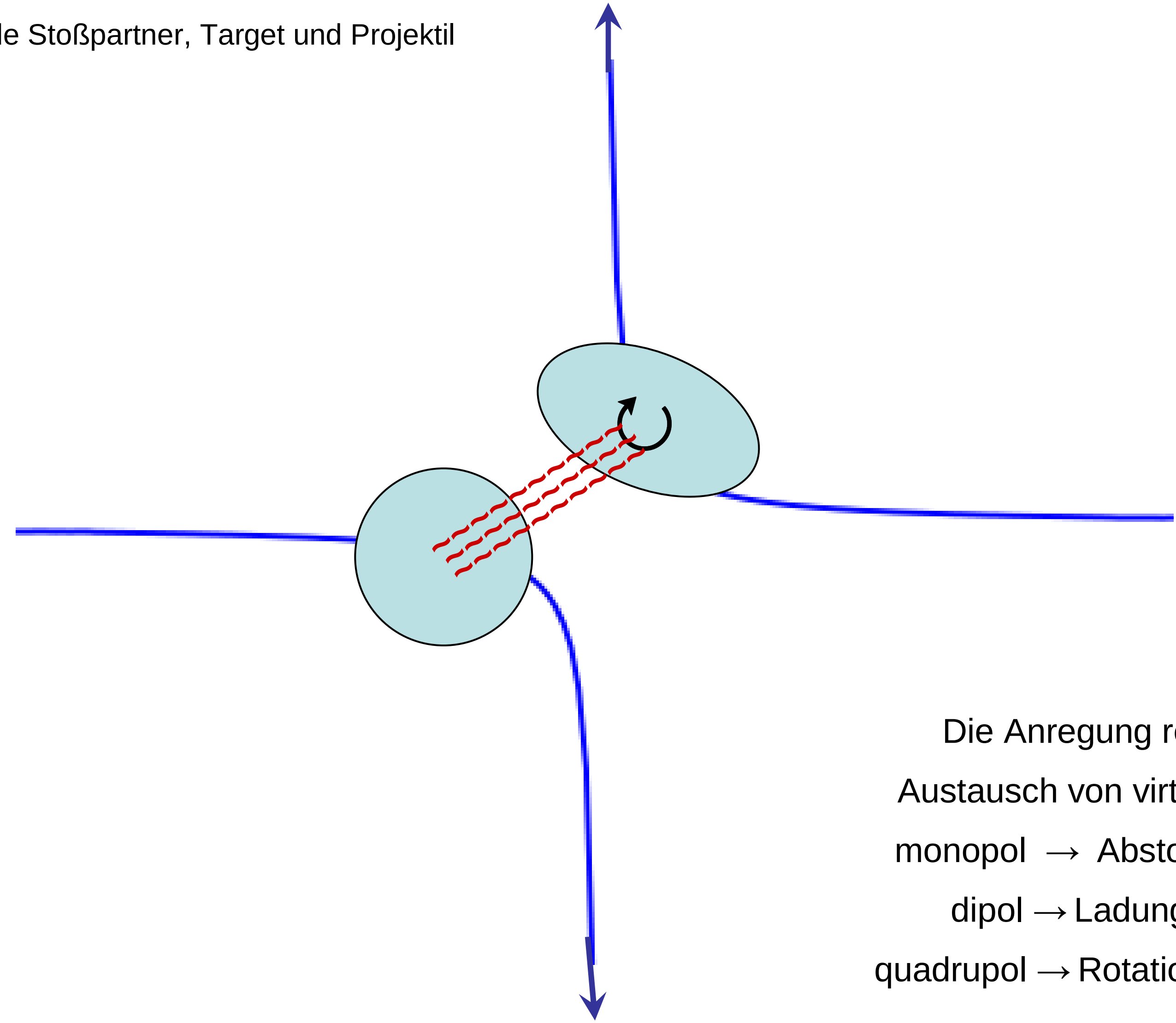

Die Anregung resultiert aus dem
Austausch von virtuellen Photonen:
monopol $\rightarrow$ Abstoßung $\rightarrow$ Bahn,
dipol $\rightarrow$ Ladungsschwingungen,
quadrupol $\rightarrow$ Rotation & Schwingung

Coulombanregung experimentell

im cm-Sytem, angeregt werden können
beide Stoßpartner, Target und Projektil

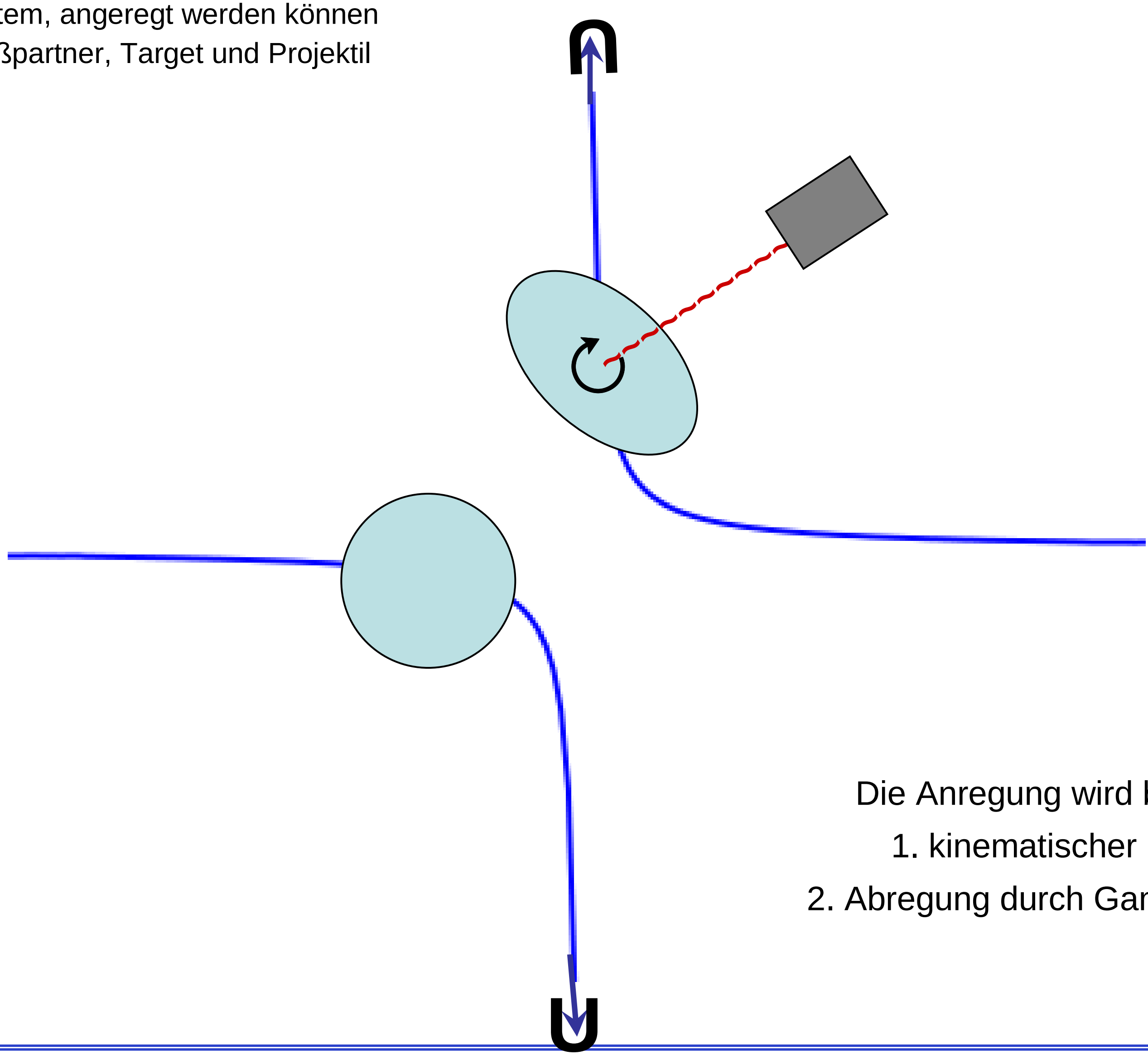

Die Anregung wird beobachtet als:

1. kinematischer Energieverlust,
2. Abregung durch Gamma-Emission,

oder

Coulombanregung experimentell

im cm-Sytem, angeregt werden können
beide Stoßpartner, Target und Projektil

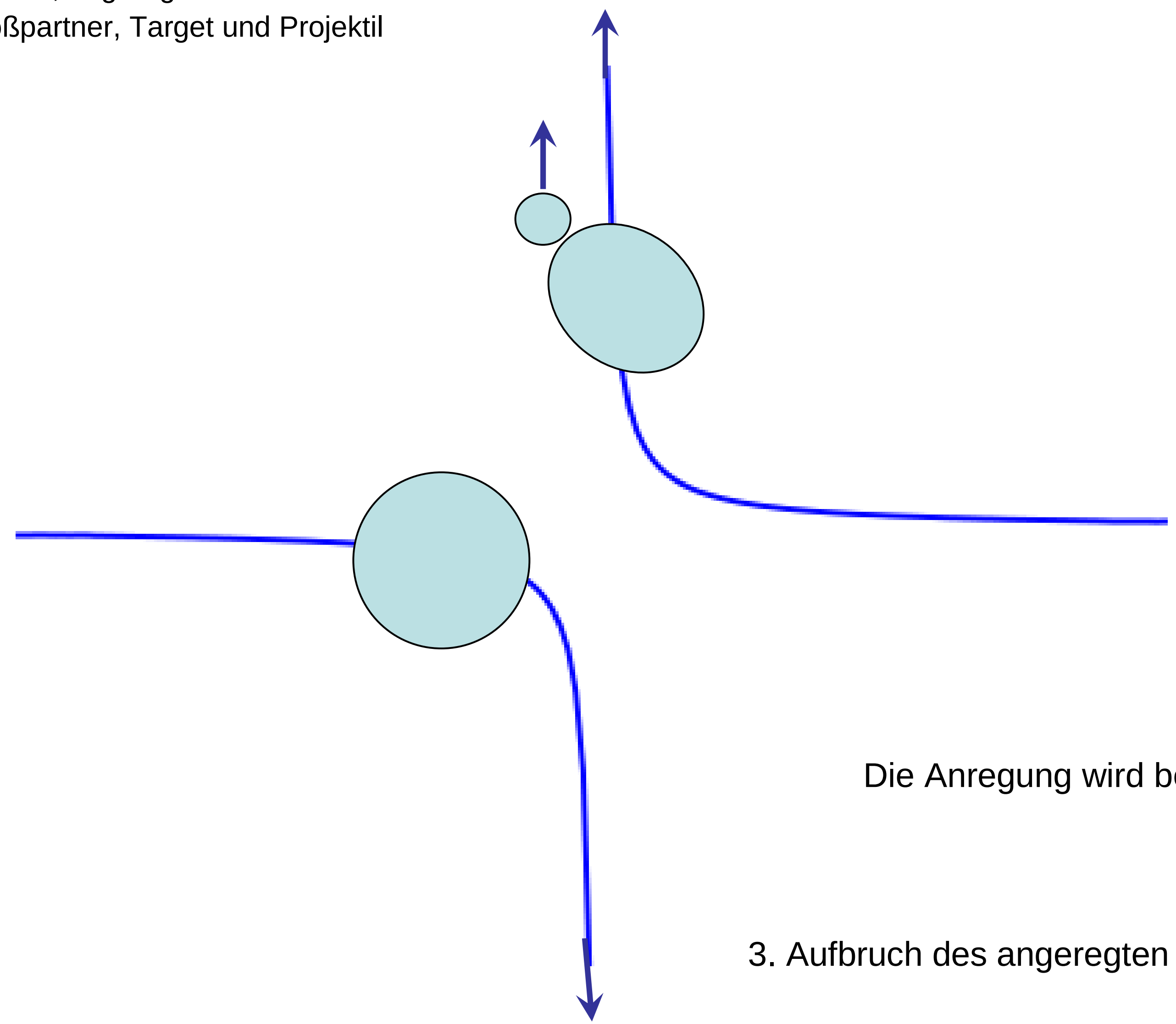

Die Anregung wird beobachtet als:

3. Aufbruch des angeregten Stoßpartners

R3B: Flugzeitanlage zur Messung geladener und neutraler Produkte aus Kernreaktionen mit radioaktiven Ionenstrahlen an FAIR

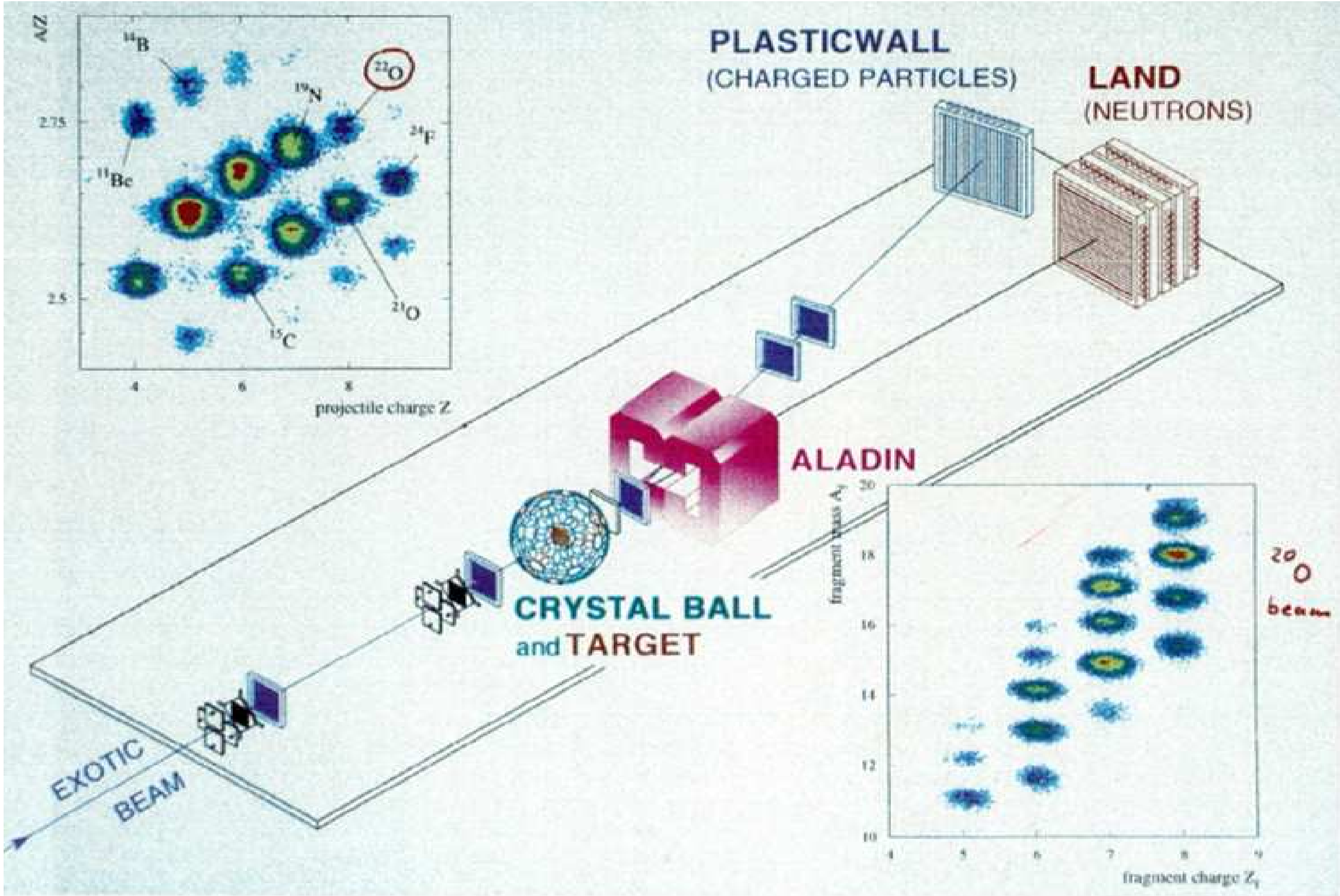

Photo-Anregung

durch reelle Photonen
z.B. aus Bremsstrahlung

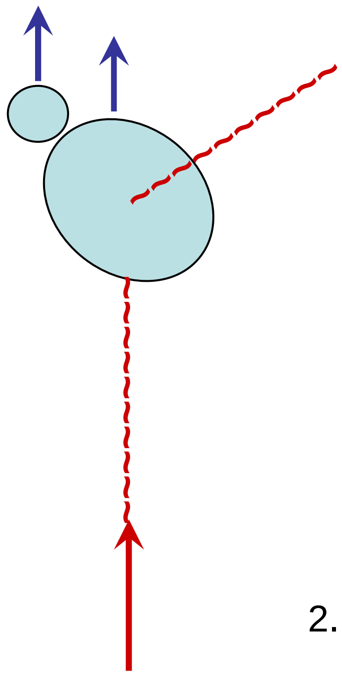

Die Anregung wird beobachtet als:

1. Photonen-Energieverlust,
2. Abregung durch verzögerte Emission,

oder

3. Aufbruch des angeregten Stoßpartners,
in den meisten Fällen ein Neutron

→ (γ,n)-Prozess

Decay rates T, widths Γ, reduced transition probabilities and cross sections for Coulomb excitation and photon absorption

$$\Gamma = \frac{\hbar}{\lambda} = \hbar \cdot \mathrm{T} = \frac{8\pi(\lambda+1)}{\lambda\{(2\lambda+1)!!\}^2} \left(\frac{E}{\hbar c}\right)^{2\lambda+1} B(\Pi\lambda) \;\; ; \;\; B(\Pi\lambda, J_{\mathrm{i}} \rightarrow J_{\mathrm{j}}) = \frac{\left|\left\langle J_{\mathrm{i}} \| \Pi\lambda \| J_{\mathrm{j}} \right\rangle\right|^2}{(2J_{\mathrm{i}}+1)^{2\lambda-1}};$$

$$\Pi : E \; or \; M$$

Coulomb excitation

$$\sigma_{Cx} = \frac{(2Z_1 Z_2 mc^2 \alpha\hbar c)^2}{(qc)^4} \cdot P_{ij} = \sigma_{Ruth} \cdot \frac{\alpha}{\beta^2} \cdot \frac{16\pi^2 \cdot Z_1^2}{(2\lambda+1)^3} \cdot \frac{B(E\lambda)}{a^{2\lambda} \cdot \hbar c} \cdot \sum_{\mu} \left|Y_{\lambda\mu}\right|^2 \cdot \left|I_{\lambda\mu}\right|^2$$

m: *reduced mass*, α: *fine structure const.*, a: *½ dist of closest approach*

Photon absorption, $\Gamma = \Gamma_\gamma$

from J_0=0 into J_1=1

$$\sigma_{abs} = \sigma_0 \frac{E^2\Gamma^2}{(E_0{}^2 - E^2)^2 + E^2\Gamma^2} \qquad \sigma_0 = 2 \cdot \frac{2J_1+1}{2J_0+1} \frac{\pi \cdot (\hbar c)^2}{E_R{}^2} \cong 73b \quad @\, 10.0\; MeV$$

Absorption integral over upper level $\int \sigma_{abs}(E)dE \cong \frac{\pi}{2} \cdot \sigma_0 \cdot \Gamma \propto B(\Pi\lambda)$

Absorption (or emission) of dipole radiation by an oscillator (Jackson, p.804):

$$\sigma_{abs} = \sigma_0 \cdot \frac{E^2 \cdot \Gamma_\gamma \Gamma}{(E_o{}^2 - E^2 + \Gamma^2/4)^2 + E^2\Gamma^2} \cong \sigma_0 \cdot \frac{E^2 \cdot \Gamma_\gamma \Gamma}{(E_R{}^2 - E^2)^2 + E^2\Gamma^2}$$

Lorentz curve

$$\approx \sigma_0 \cdot \frac{\Gamma_\gamma \Gamma}{4(E_R - E)^2 + \Gamma^2} \cdot \frac{E}{E_R} \quad \Rightarrow \quad \sigma_o = \frac{6\pi \cdot \hbar^2 c^2}{E_R{}^2} = 7.3 \cdot 10^{+3}\ fm^2 = 73\ b$$

Breit-Wigner form

unitarity limit for $E_R = 10$ MeV

resonant process, $\tau \sim \hbar/\Gamma > 10^{-16}$s

Thompson scattering of photons from a charged point particle (Jackson, p.682):

$$\sigma_{sc} = \frac{8\pi \cdot \alpha\hbar c}{3} \cdot \frac{Z^2}{A m_N c^2} = 6.2 \cdot 10^{-3}\ fm^2 = 62\,\mu b$$

for Mo

direct process, $t \sim R/c \sim 10^{-23}$s

Der Rutherfordquerschnitt und die elektroschwache Wechselwirkung,
eine Lorentz-Kurve bei 0 und eine bei Z_0

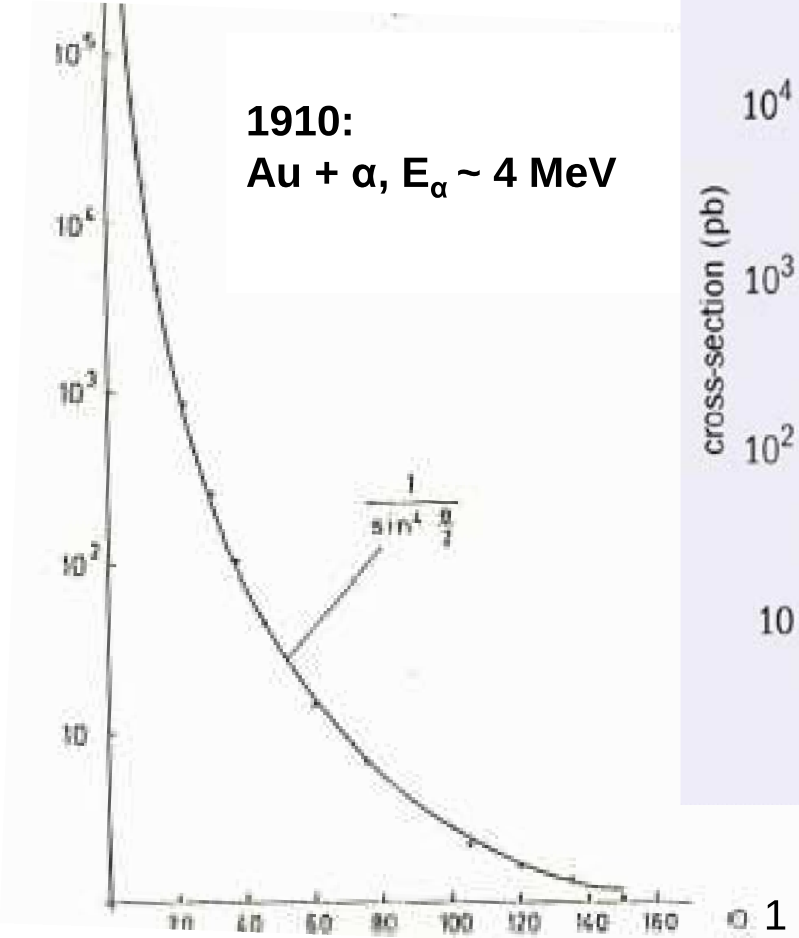

1910:
Au + α, E_α ~ 4 MeV

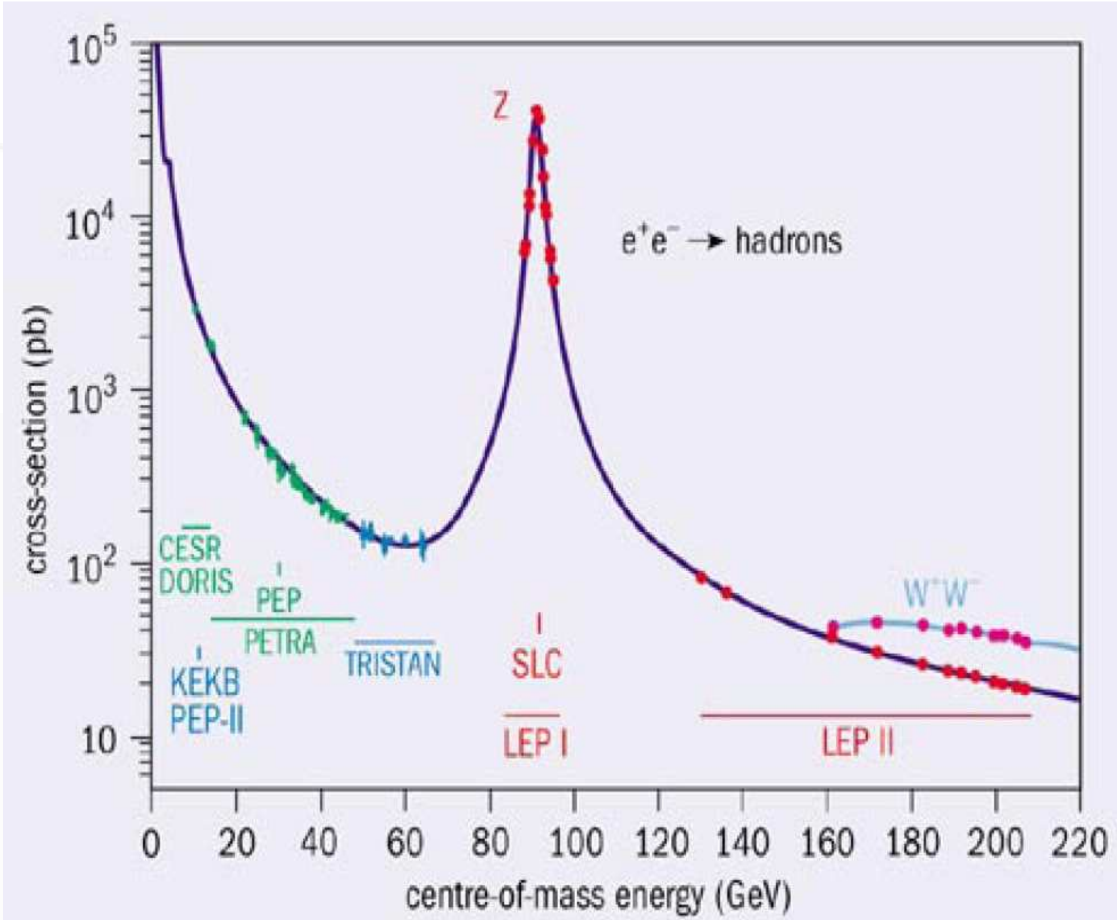

1990: $e^+e^- \rightarrow$ hadrons **von < 10 bis >100 GeV**

A. Bohr & B. Mottelson, Nuclear Structure – Dipole Modes

The <u>G</u>iant <u>D</u>ipole <u>R</u>esonance in ^{197}Au and a fit with the modified Breit-Wigner formula

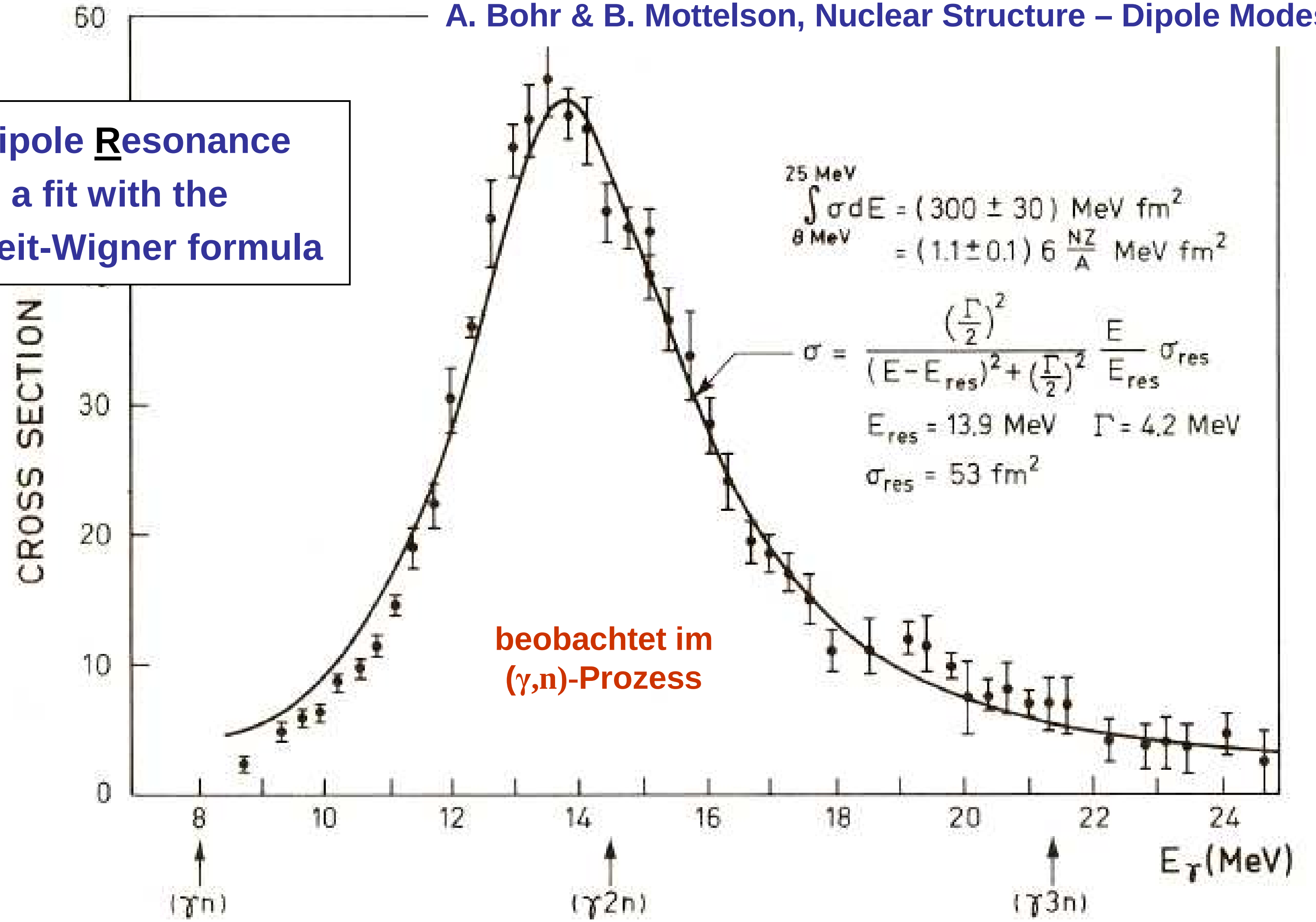

Figure 6-18 Total photoabsorption cross section for ^{197}Au. The experimental data are from S. C. Fultz, R. L. Bramblett, J. T. Caldwell, and N. A. Kerr, *Phys. Rev.* **127**, 1273 (1962). The solid curve is of Breit-Wigner shape with the indicated parameters.

Two ways to look at heavy nuclei and their giant resonances

microscopic – quantum-mechanical:
shell model of nucleons in mean field
particle - hole excitations

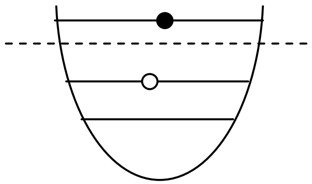

particle – hole excitations
across a major shell ⇒ $J^{\pi} = 1^{-}$

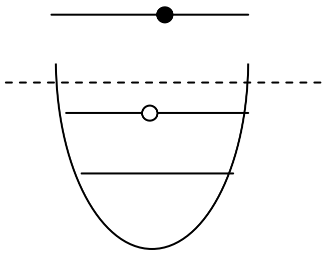

Brown & Bolsterli

nucleus
at low energy

GDR:
giant dipole resonance

theory ~ 1950

Steinwedel & Jensen

macroscopic – phenomenological:
liquid drop model → droplet model
rotations & vibrations

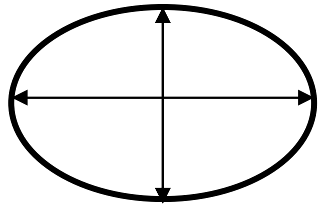

protons and neutrons oscillate
against each other

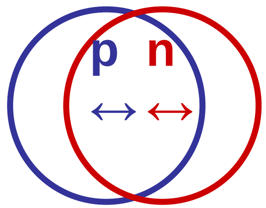

Goldhaber & Teller

Tamm-Dankoff → RPA → QRPA → def'd RPA → QPM → Dynamic Collective Model

Collective models for the GDR

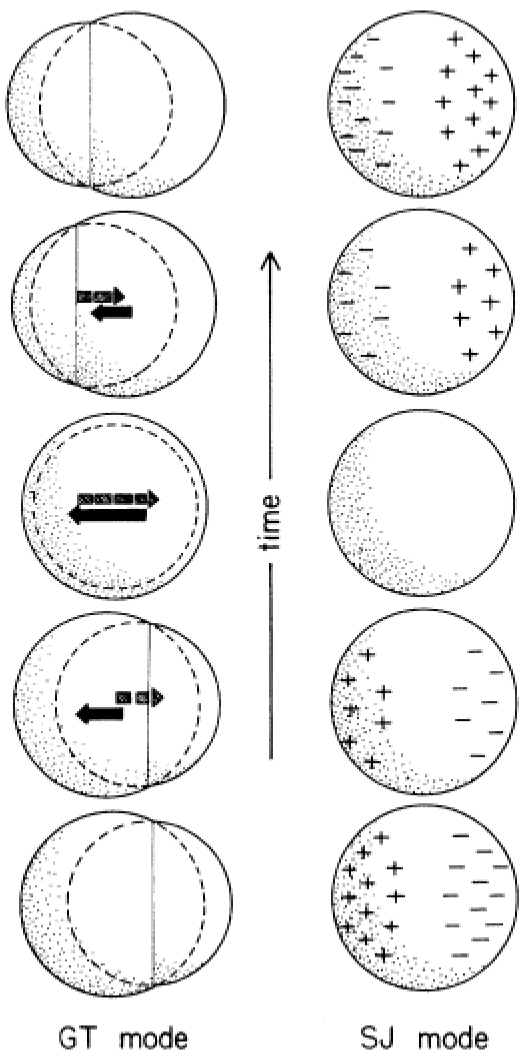

Goldhaber+Teller *Steinwedel+Jensen*

Droplet model with compressibility and symmetry-energy

W. D. Myers et al., PRC 15 (1977) 2032

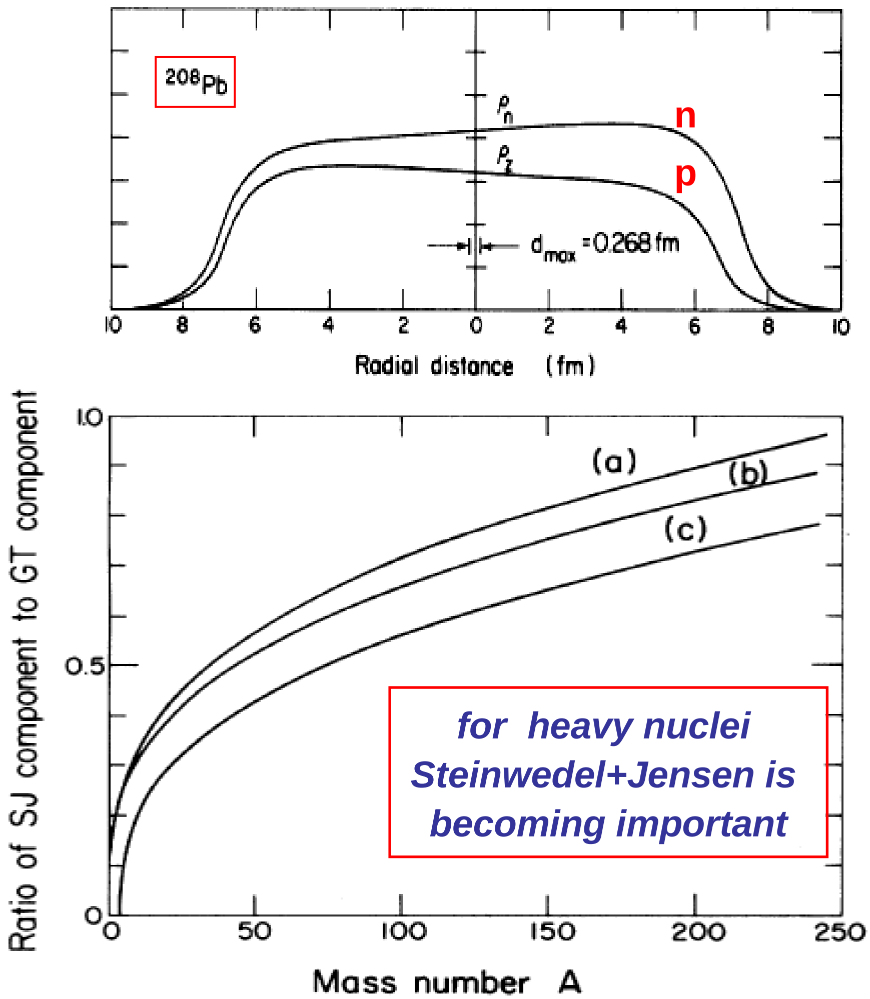

	^{142}Nd	^{144}Nd	^{146}Nd	^{148}Nd	^{150}Nd	
E_0(MeV)	14.9	15.0	14.8	14.7	12.3	16
σ_0(fm^2)	36	32	31	26	17	22
Γ(MeV)	4.4	5.3	6	7.2	3.3	5.2

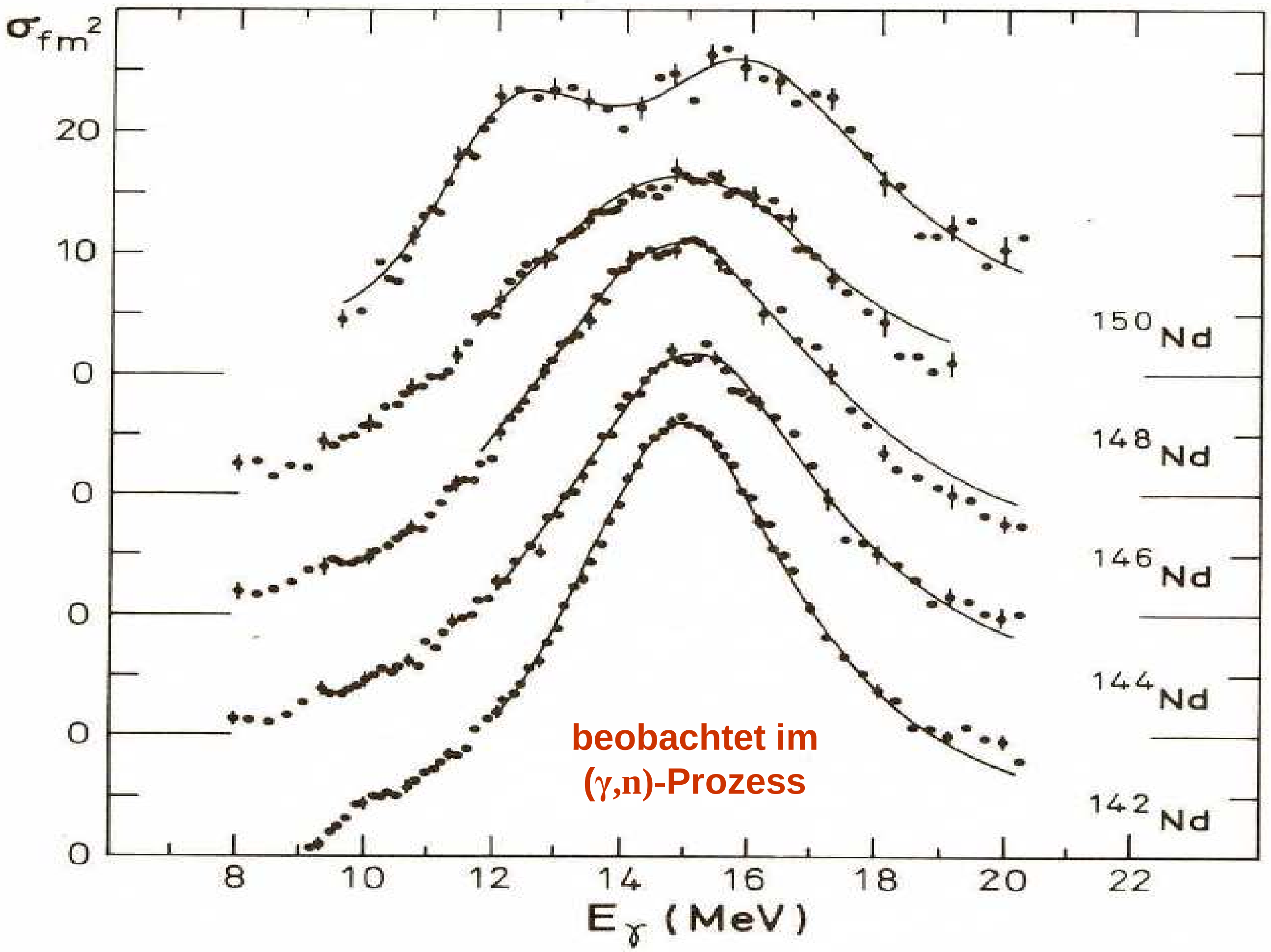

beobachtet im
(γ,n)-Prozess

axially deformed

spherical

A. Bohr & B. Mottelson, Structure of Nuclei – Dipole Modes

Beschreibung der Riesenresonanz mit der Dichte-Funktional-Methode

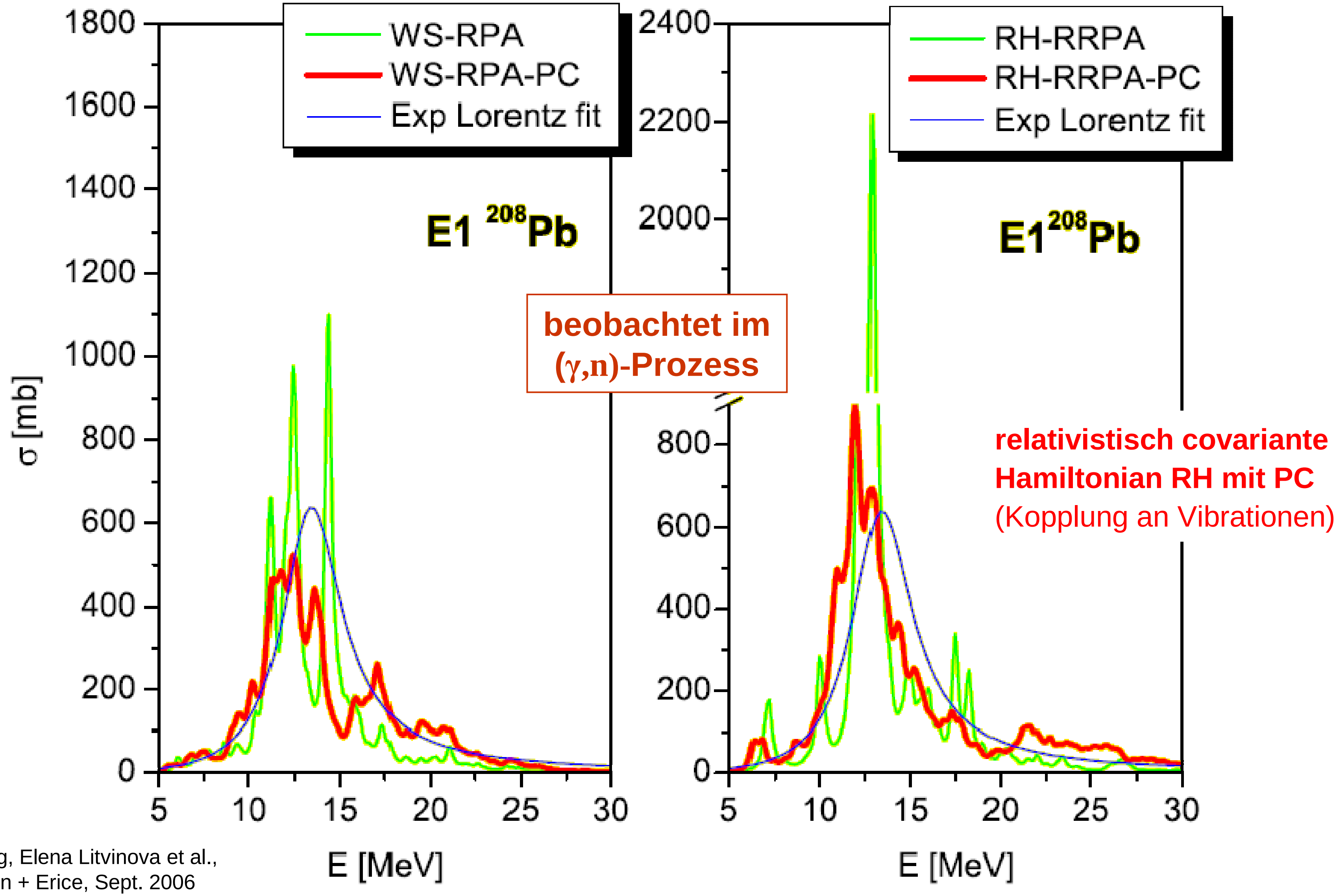

Peter Ring, Elena Litvinova et al.,
München + Erice, Sept. 2006

To study the e.m. properties of a nucleus' excited state i one can:

1. **insert the nucleus in an e.m- field $\Rightarrow \mu_i$, Q_i**
2. **excite it by an electron or fast ion (virtual photon, Coulex,..)**
3. **use a photon beam (e.g. from ELBE.., $\Gamma_{\gamma i} > 0.1$ eV)**
4. **excite it hadronically and measure e.m. decay probability:**
   - **a. electronically (τ_i > ns, $\hbar/\tau_i \approx \mu$eV)**
   - **b. recoil distance Doppler shift ($\tau_i \approx$ ps, $\hbar/\tau_i \approx$ meV)**
   - **c. Doppler shift attenuation (τ_i >10 fs, $\hbar/\tau_i < 0.1$ eV)**

Only Coulex can deliver $\gamma_{\gamma i}$ with sign, the other methods give $\Gamma_\gamma = \gamma_\gamma^2$

5. excite and measure branching ratio for comparison to Γ_i known from:
   - a. p-capture calculation (statistical model)
   - b. high resolution tof total n cross section; if $\Gamma_n \ll \Gamma_\gamma$ then $\Gamma_{\gamma i} \approx \Gamma_i \approx 0.1$ eV
   - c. n-capture yield; if $\Gamma_\gamma \ll \Gamma_n$ $\longrightarrow \int \sigma(n,\gamma)\, dE \propto \Gamma_n \cdot \Gamma_\gamma / \Gamma \approx \Gamma_\gamma$,

     and n-transmission $\longrightarrow \int \sigma(n,n)\, dE \propto \Gamma_n^2/\Gamma \approx \Gamma_n$. $\quad \Gamma_n + \Gamma_\gamma = \Gamma$

Planck-Strahlung
im Sichtbaren

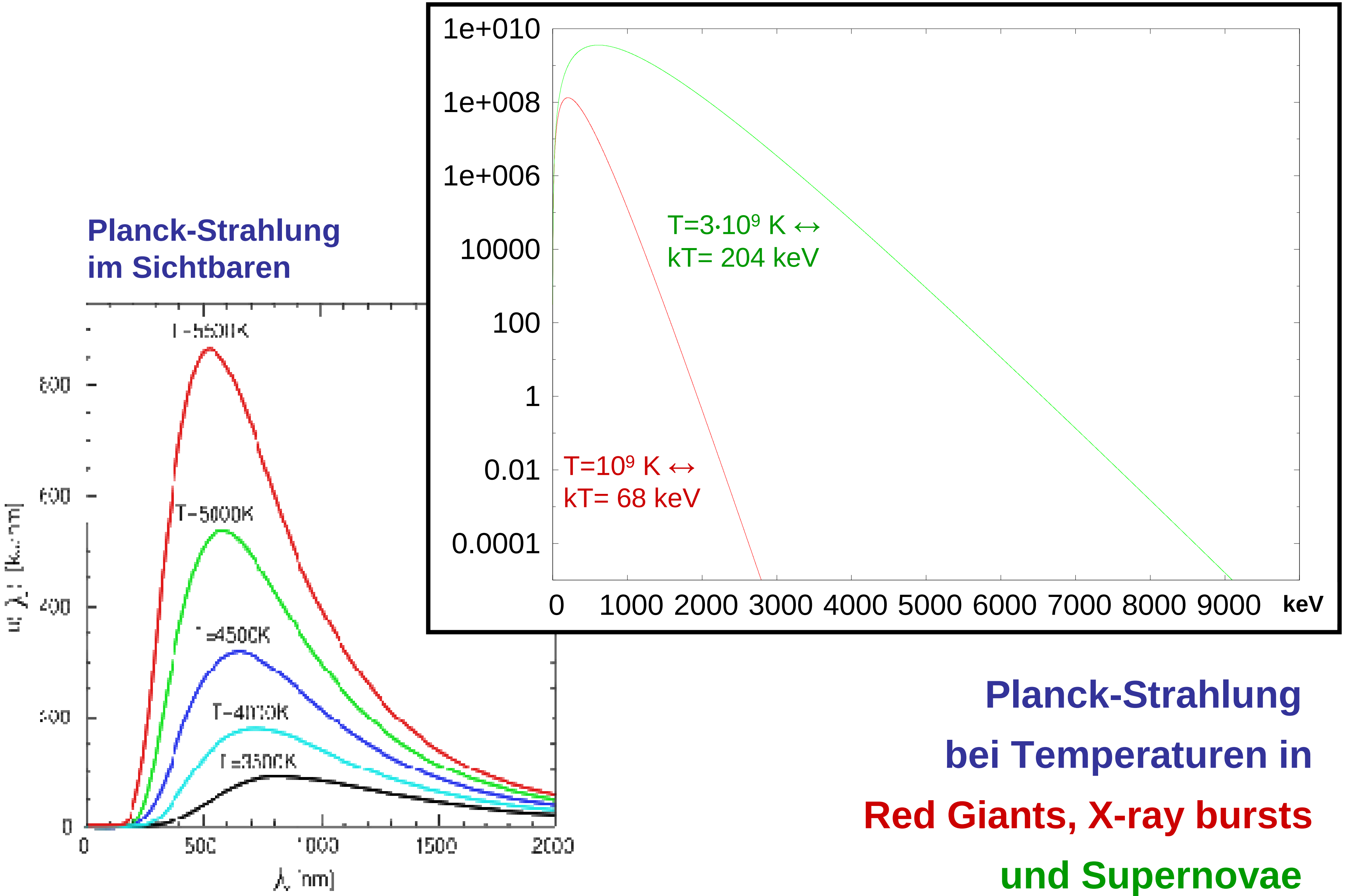

nach Wikipedia®

Planck-Strahlung

bei Temperaturen in

Red Giants, X-ray bursts

und Supernovae

Nukleosynthese und Bindungsenergie

$E_B = (\Delta m \cdot c^2)$; $\Delta m = Z \cdot m_p + N \cdot m_n - m_{Kern}$

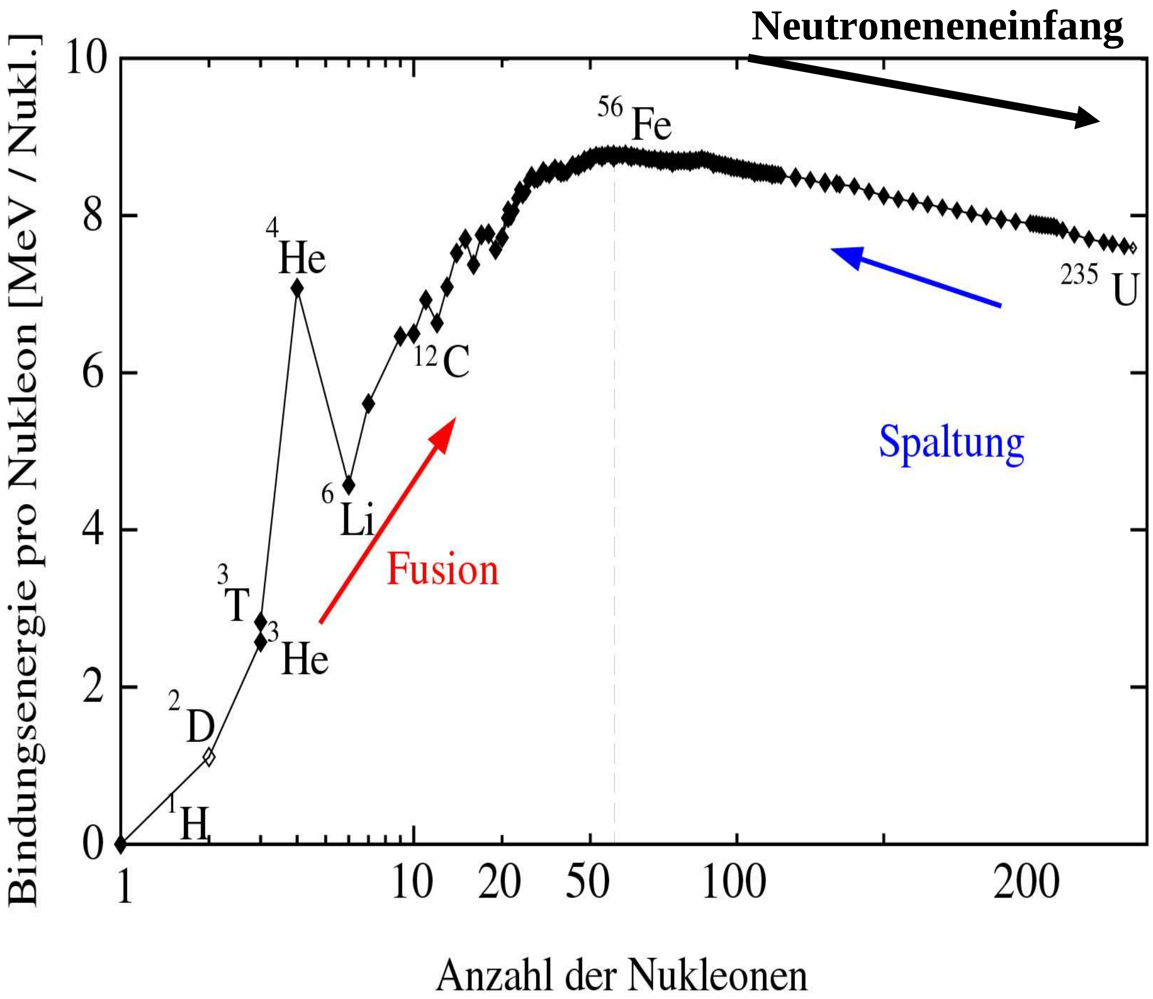

Kernfusion ohne Energiezufuhr ist nur möglich bis zum Eisen.

Schwerere Kerne können wg. elektrischerAbstoßung nur durch Neutroneneinfang-Prozesse gebildet werden.

Sehr schwere Kerne können spontan spalten; durch die Kernkraft wird die Spaltung aber behindert.

Die Häufigkeit der Elemente im Sonnensystem

Wasserstoff : $^1H = p$	X = 0.70
Helium : $^4He = \alpha$	Y = 0.28
Alle anderen Nuklide	Z = 0.019
Schwere Elemente (> Ni)	$4*10^{-6}$